(12) INTERNATIONAL APPLICATION PUBLISHED UNDER THE PATENT COOPERATION TREATY (PCT)

(19) World Intellectual Property Organization
International Bureau

(43) International Publication Date
20 June 2013 (20.06.2013)

WIPO | PCT

(10) International Publication Number
WO 2013/090770 A2

(51) International Patent Classification:
A61K 38/16 (2006.01)

(21) International Application Number:
PCT/US20 12/06983 1

(22) International Filing Date:
14 December 2012 (14. 12.2012)

(25) Filing Language: English

(26) Publication Language: English

(30) Priority Data:
61/570,620 14 December 201 1 (14. 12.201 1) US
61/596,869 9 February 2012 (09.02.2012) US

(71) Applicants: **THE BOARD OF TRUSTEES OF THE UNIVERSITY OF ARKANSAS** [US/US]; 2404 North University Avenue, Little Rock, AR 72207 (US). **KITASATO UNIVERSITY** [JP/JP]; 1-15-1 Sagamihara-shi, Minamin-ku, Kanagawa, 252-0374 (JP). **MONTEFIORE MEDICAL CENTER** [US/US]; 3415 Bainbridge Avenue, Bronx, NY 10467 (US).

(72) Inventors: **SAKON, Joshua;** 207 Skyline Drive, Fayetteville, AR 72701 (US). **PHILOMINATHAN, Sagaya, Theresa, Leena;** 103 Greens Loop, Cheshire, CT 06410 (US). **KATIKANENI, Ranjitha;** 5615 Netherlands Avenue, #ld, Bronx, NY 10471-1700 (US). **MATSUSHITA, Osamu;** 3-2-1 Chiyoda, Apt. 203, Chuo-ku, Sagamihara, Kanagawa, 252-0237 (JP). **PONNAPAKKAM, Tulasi;** 5615 Netherlands Avenue, #ld, Bronx, NY 10471-1700 (US). **KOIDE, Takaki;** Waseda University Shinjuku-ku, Tokyo, 169-8555 (JP). **CENSURE, Robert, C ;** 341 5 Bainbridge Avenue, Room 107, Bronx, NY 10467 (US).

(74) Agents: **VANHEYNINGEN, Tambryn, K.** et al; Andrus, Sceales, Starke & Sawall, LLP, 100 East Wisconsin Avenue, Suite 1100, Milwaukee, WI 53202 (US).

(81) Designated States *(unless otherwise indicated, for every kind of national protection available):* AE, AG, AL, AM, AO, AT, AU, AZ, BA, BB, BG, BH, BN, BR, BW, BY, BZ, CA, CH, CL, CN, CO, CR, CU, CZ, DE, DK, DM, DO, DZ, EC, EE, EG, ES, FI, GB, GD, GE, GH, GM, GT, HN, HR, HU, ID, IL, IN, IS, JP, KE, KG, KM, KN, KP, KR, KZ, LA, LC, LK, LR, LS, LT, LU, LY, MA, MD, ME, MG, MK, MN, MW, MX, MY, MZ, NA, NG, NI, NO, NZ, OM, PA, PE, PG, PH, PL, PT, QA, RO, RS, RU, RW, SC, SD, SE, SG, SK, SL, SM, ST, SV, SY, TH, TJ, TM, TN, TR, TT, TZ, UA, UG, US, UZ, VC, VN, ZA, ZM, ZW.

(84) Designated States *(unless otherwise indicated, for every kind of regional protection available):* ARIPO (BW, GH, GM, KE, LR, LS, MW, MZ, NA, RW, SD, SL, SZ, TZ, UG, ZM, ZW), Eurasian (AM, AZ, BY, KG, KZ, RU, TJ, TM), European (AL, AT, BE, BG, CH, CY, CZ, DE, DK, EE, ES, FI, FR, GB, GR, HR, HU, IE, IS, IT, LT, LU, LV, MC, MK, MT, NL, NO, PL, PT, RO, RS, SE, SI, SK, SM, TR), OAPI (BF, BJ, CF, CG, CI, CM, GA, GN, GQ, GW, ML, MR, NE, SN, TD, TG).

Published:

— *without international search report and to be republished upon receipt of that report (Rule 48.2(g))*

— *with sequence listing part of description (Rule 5.2(a))*

(54) Title: DELIVERY OF THERAPEUTIC AGENTS BY A COLLAGEN BINDING PROTEIN

Figure 1

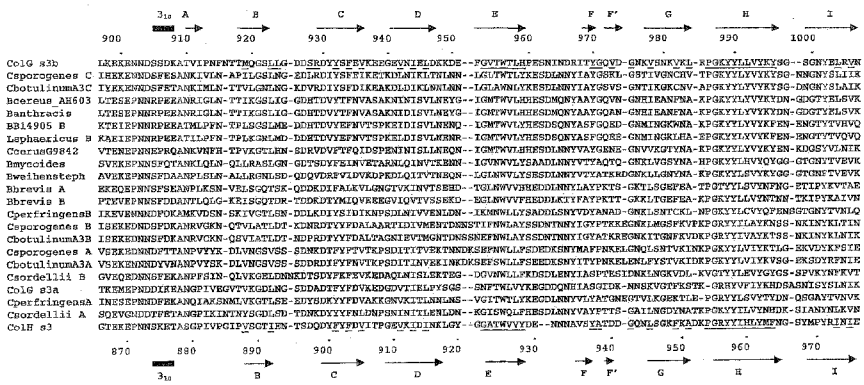

(57) Abstract: Methods of delivering therapeutic agents by administering compositions including a bacterial collagen-binding polypeptide segment linked to the therapeutic agent to subjects in need of treatment with the therapeutic agent are provided. In these methods, the therapeutic agent is not a PTH/PTHrP receptor agonist or antagonist, basic fibroblast growth factor (bFGF) or epidermal growth factor (EGF). The bacterial collagen-binding polypeptide segment delivers the agent to sites of partially untwisted or under-twisted collagen. Methods of treating collagenopathies using a composition including a collagen-binding polypeptide and a PTH/PTHrP receptor agonist are also provided. In addition, methods of treating hyperparathyroidism, and hair loss using compositions comprising a collagen binding polypeptide and a PTH/PTHrP receptor agonist are provided. Finally, methods of reducing hair regrowth by administering a composition including a collagen binding polypeptide and a PTH/PTHrP receptor antagonist are provided.

DELIVERY OF THERAPEUTIC AGENTS BY A COLLAGEN BINDING PROTEIN

CROSS-REFERENCE TO RELATED APPLICATIONS

This patent application claims the benefit of priority of United States Provisional Patent Application No. 61/570,620, filed December 14, 201 1 and of United States Provisional Patent Application No. 61/596,869, filed February 9, 2012, both of which are incorporated herein by reference in their entireties.

STATEMENT REGARDING FEDERALLY SPONSORED RESEARCH

This invention was made with United States government support awarded by the National Institutes of Health grant number NCRR COBRE 8P30GM103450 and INBRE GM103429. The United States may have certain rights in this invention.

SEQUENCE LISTING

A Sequence Listing accompanies this application and is incorporated herein by reference in its entirety. The Sequence Listing was filed with the application as a text file on December 14, 2012.

INTRODUCTION

Delivery of therapeutic agents to sites within the body of a subject where a particular therapeutic agent is needed in order to be effective is a developing area. Such delivery systems will allow more efficient use of therapeutic agents while reducing toxicity caused by some therapeutic agents. Use of targeted liposomes or polypeptides, such as antibodies, to target therapeutic agents to particular sites within the body has proved successful, but additional delivery agents are needed.

Alopecia (hair loss) is a psychologically and emotionally distressing event with multiple causes. Alopecia occurs most commonly in male-pattern baldness, affecting approximately two thirds of males by age 35; a similar pattern of hair loss can be observed in females with polycystic ovarian syndrome. In both of these disorders, the hair loss is androgen mediated. Alopecia can also occur as an autoimmune disease, termed alopecia areata; a disorder which affects 1.7% of the population. It can occur as a side-effect of medical treatments, particularly in

chemotherapy, with 65-85% of chemotherapy patients experiencing some degree of alopecia. Psychological consequences of hair loss have been well studied in the chemotherapy setting. Chemotherapy-induced alopecia (CIA) can result in anxiety, depression, a negative body image, lowered self-esteem and a reduced sense of well-being. In fact, 47-58% of female cancer patients consider hair loss to be the most traumatic aspect of chemotherapy, and 8% would decline treatment for fear of hair loss. In addition to these studies in chemotherapy patients, evidence exists in other forms of alopecia to support therapy to reduce psychological consequences of hair loss. Thus a new treatment to stop hair loss or speed hair regrowth would be beneficial.

While drugs with mild anti-androgenic effects (i.e. spironolactone) had been used with limited success as therapy for alopecia, the first effective medication for alopecia was minoxidil (Rogaine). This antihypertensive has an observed side-effect of causing hair growth, and is now used as topical therapy for many forms of alopecia. However, responses are incomplete, with some subjects showing only slowing of hair loss rather than actual regrowth. Finasteride (Propecia) is a newer agent that blocks conversion of testosterone to dihydrotestosterone, resulting in improvements in androgenic alopecia at the expense of partial systemic androgen blockade. However, response rates with long-term (10 years) therapy are only around 50%. Overall, despite considerable research in this area, there is still no adequate therapy for hair loss.

In addition, unwanted hair growth is a cosmetic issue many people deal with on a regular basis. Unwanted hair growth on the face, legs, arms, chest or back is a growing cosmetic problem. Many people use laser therapy, waxing or other therapies to remove unwanted hair. There are currently no topical pharmaceuticals to limit hair growth.

Collagenopathies represent a large number of diseases in which collagen structure or formation is not normal. This group of diseases results in a broad spectrum of symptoms including bone defects, vascular defects, and skin defects. Many of these diseases have no or only ineffective treatments available.

For example, osteogenesis imperfecta (OI), also known as brittle bone disease, is caused by an inborn mutation of type I collagen. Approximately 25,000 to 50,000 Americans are affected and the effects of the disease range from mild, in which many individuals are unaware of the disease, to severe in which individuals cannot live a normal life due to recurrent broken bones. Most OI patients carry a mutation which causes an amino acid change in collagen

changing a glycine to a bulkier amino acid which results in disruption of the triple helix structure of the collagen and under-twisting. The body may respond by hydrolyzing the collagen and this may result in a reduction in bone strength. There is currently no cure and few treatments for 01.

SUMMARY

Provided herein are methods of delivering therapeutic agents by administering compositions including a bacterial collagen-binding polypeptide segment linked to the therapeutic agent to subjects in need of treatment with the therapeutic agent. In these methods, the therapeutic agent is not a PTH/PTHrP receptor agonist or antagonist, basic fibroblast growth factor (bFGF) or epidermal growth factor (EGF) and the bacterial collagen-binding polypeptide segment delivers the agent to sites of partially untwisted or under-twisted collagen.

In another aspect, methods of treating a subject with a collagenopathy, such as osteogenesis imperfecta, by administering a composition comprising a bacterial collagen-binding polypeptide segment linked to a PTH/PTHrP receptor agonist to a subject in an amount effective to treat the collagenopathy are provided. The bacterial collagen-binding polypeptide segment delivers the agent to sites of partially untwisted or under-twisted collagen.

In yet another aspect, methods of treating hyperparathyroidism by administering a composition comprising a bacterial collagen-binding polypeptide segment linked to a PTH/PTHrP receptor agonist to a subject are provided.

In still a further aspect, methods of slowing hair growth or regrowth after removal by administering a composition comprising a bacterial collagen-binding polypeptide segment linked to a PTH/PTHrP receptor antagonist to a subject are provided.

In a still further aspect, methods of increasing hair growth or the speed of hair re-growth after removal or loss by administering a composition comprising a bacterial collagen-binding polypeptide segment linked to a PTH/PTHrP receptor agonist to a subject are provided.

BRIEF DESCRIPTION OF THE DRAWINGS

Figure 1 is a sequence alignment showing the alignment of several M9B bacterial collagenases from the Bacillus and Clostridium families. The residues shown in blue are important for collagen binding activity, those shown in green are important for maintaining the architecture or protein folding. Both of these are also underlined for the top and bottom

sequences. Residues shown in red are critical for Ca^{2+} binding and those in orange are critical for positioning the Ca^{2+} binding residues.

Figure 2 is a set of drawings showing the chemical structures of synthesized peptides.

Figure 3A is a graph showing the circular dichroism spectra of the collagenous peptides measured at 4°C.

Figure 3B is a graph showing the thermal denaturation profile of the various collagenous peptides. The temperature was increased at the rate of 0.3°C/min.

Figure 4A is a graph showing the scattering profile with the intensity I(Q) plotted against the scattering vector Q.

Figure 4B is a graph showing the pair-distance distribution function P(r) in the real space obtained using GNOM for [PROXYL-$(POG)_3POA(POG)_6]_3$:CBD complex (Red), [PROXYL-$(POG)_4POA(POG)_5]_3$:CBD complex (Blue), [PROXYL-$(POG)_5POA(POG)_4]_3$:CBD complex (Green), [PROXYL-$(POG)_6POA(POG)_3]_3$:CBD complex (Orange) and [1lPROXYL-$(POG)_3PCG(POG)_4]_3$:CBD complex (Cyan).

Figure 5 is a set of plots showing HSQC NMR data obtained using the collagen binding domain (CBD) - collagenous peptide interactions. Figure 5A shows an overlay of ^{1}H-^{15}N HSQC spectrum of CBD (black) and ^{1}H-^{15}N HSQC spectrum of $[(POG)_{10}]_3$:CBD complex (green) at 1:1 ratio. Amide resonance of V973, G975 and S979 are present during this titration. Figure 5B shows an overlay of ^{1}H-^{15}N HSQC spectrum of CBD (black) and ^{1}H-^{15}N HSQC spectrum of [PROXYL-$(POG)_6POA(POG)_3]_3$:CBD complex (red) at 1:1 ratio. Amide resonances of V973, G975 and S979 disappeared because of their proximity to the spin-labeled group. Figure 5C is a cartoon showing the structure of CBD and the CBD residues that are line broadened upon titration with [PROXYL-$(POG)_6POA(POG)_3]_3$.

Figure 6 is a set of plots showing HSQC NMR data obtained using the CBD - collagenous peptide interactions. Figure 6A shows an overlay of ^{1}H-^{15}N HSQC spectrum of CBD (black) and ^{1}H-^{15}N HSQC spectrum of $[(POG)i_0]_3$:CBD complex (green) at 1:1 ratio. Amide resonances of Q972, V973, G975 and S979 are present during this titration. Figure 6B shows an overlay of ^{1}H-^{15}N HSQC spectrum of CBD (black) and ^{1}H-^{15}N HSQC spectrum of [PROXYL-$(POG)_5POA(POG)_4]_3$:CBD complex (red) at ratio 1:1. Amide resonances of Q972, V973, G975 and S979 are line broadened due to the PROXYL moiety. Figure 6C is a cartoon of the structure of CBD showing the CBD residues that are uniquely line broadened upon titration

with [PROXYL-$(POG)_5$POA$(POG)_4$]3. Figure 6D shows an overlay of ^1H-^{15}N HSQC spectrum of CBD (black) and ^1H-^{15}N HSQC spectrum of [$(POG)i_0]_3$:CBD complex (green) at 1:1 ratio. Amide resonances of L946, Q972, V973, G975 and S979 are present during this titration. Figure 6E shows an overlay of ^1H-^{15}N HSQC spectrum of CBD (black) and ^1H-^{15}N HSQC spectrum of [PROXYL-$(POG)_4$POA$(POG)_5]_3$:CBD complex (red) at 1:1 ratio. Amide resonances of L946, Q972, V973, G975 and S979 disappeared because of the spin-label. Figure 6F shows an overlay of ^1H-^{15}N HSQC spectrum of CBD (black) and ^1H-^{15}N HSQC spectrum of [$(POG)_4$POA$(POG)_5]_3$:CBD (cyan) at ratio 1:1. In the absence of spin label, amide resonances of L946, Q972, V973, G975 and S979 are not line broadened. Figure 6G shows an overlay of ^1H-^{15}N HSQC spectrum of CBD (black) and ^1H-^{15}N HSQC spectrum of [$(POG)i_0]_3$:CBD complex (green) at 1:1 ratio. Amide resonances of L946, G953, Q972, V973, D974, G975, N976, V978, S979 are present during this titration. Figure 6H shows an overlay of ^1H-^{15}N HSQC spectrum of CBD (black) and ^1H-^{15}N HSQC spectrum of [PROXYL-$(POG)_3$POA$(POG)_6]_3$:CBD complex (red) at ratio 1:1. Amide resonances of L946, G953, Q972, V973, D974, G975, N976, V978, S979 are line broadened due to the PROXYL moiety. Figure 61 is a cartoon of the structure of CBD showing the CBD residues that are line broadened by the spin label of [PROXYL-$(POG)_3$POA$(POG)_6]_3$.

Figure 7 is a set of graphs showing the intensity drop of (A) Q972, (B) G975, (C) S979 and (D) L924 on CBD as a function of increasing concentrations of mini-collagen *i.e.* $[(POG)io]_3$ (black), [PROXYL-$(POG)_6$POA$(POG)_3]_3$(red), [PROXYL-$(POG)_5$POA$(POG)_4]_3$(blue), [PROXYL-$(POG)_4$POA$(POG)_5]_3$(green), and [PROXYL-$(POG)_3$POA$(POG)_6]_3$(cyan).

Figure 8 is a set of plots showing HSQC NMR data obtained using the CBD - collagenous peptide interactions. Figure 8A shows an overlay of ^1H-^{15}N HSQC spectrum of CBD (black) and ^1H-^{15}N HSQC spectrum of [$(POG)i_0]_3$:CBD complex (green) at 1:1 ratio. Amide resonances of S906, S997 and G998 are present during this titration. Figure 8B shows an overlay of ^1H-^{15}N HSQC spectrum of CBD (black) and ^1H-^{15}N HSQC spectrum of [$(POG)_4$POA$(POG)_5$C-PROXYL$]_3$:CBD complex (red) at ratio 1:1. Amide resonances of S906, S997 and G998 are line broadened due to the PROXYL moiety. Figure 8C shows an overlay of ^1H-^{15}N HSQC spectrum of CBD (black) and ^1H-^{15}N HSQC spectrum of [$(POG)_4$POA$(POG)_5$C-carbamidornethyl$]_3$:CBD (cyan) at 1:1 ratio. In the absence of spin label, amide resonances of S906, S997 and G998 are not line broadened. Figure 8D is a cartoon of the structure of CBD

showing the CBD residues that are line broadened due to the spin label of $[(POG)_4POA(POG)_5C\text{-}PROXYL]_3$. Amide resonances of S906, S997 and G998 (red) disappeared upon titration with $[(POG)_4POA(POG)_5\text{-}PROXYL]_3$. Figure 8E shows an overlay of $^1H\text{-}^{15}N$ HSQC spectrum of CBD (black) and $^1H\text{-}^{15}N$ HSQC spectrum of $[(POG)_{,0}]_3$:CBD complex (green) at 1:1 ratio. Amide resonances of S906, Q972, V973, G975, S979, S997 and G998 are present during this titration. Figure 8F shows an overlay of $^1H\text{-}^{15}N$ HSQC spectrum of CBD (black) and $^1H\text{-}^{15}N$ HSQC spectrum of [1 1PR0XYL-(P0G)$_3$PCG(P0G)$_4$]$_3$:CBD complex (red) **at** 1:1 ratio. Amide resonances of S906, Q972, V973, G975, S979, S997 and G998 disappeared because of the spin-label. Figure 8G shows an overlay of $^1H\text{-}^{15}N$ HSQC spectrum of CBD (black) and $^1H\text{-}^{15}N$ HSQC spectrum of $[(POG)_3PCG(POG)_4]_3$:CBD (cyan) at ratio of 1:1. Resonances of S906, Q972, V973, G975, S979, S997 and G998 are intact in the absence of the spin label. Figure 8H is a cartoon of the structure of CBD showing the residues that are line broadened upon titration with [1 1PROXYL- $(POG)_3PCG(POG)_4]_3$. Only amide resonances of S906, R929, S997, and G998 (red) disappeared at 0.2:1 ratio. When the peptide ratio was raised to 0.3:1, additional resonances of V973, G975, S979 (blue) disappeared.

Figure 9 is a set of structure drawings derived from SAXS scattering profiles using *ab initio* simulated annealing calculations for (A) $[PROXYL\text{-}(POG)_3POA(POG)_6]_3$:CBD complex, (B) $[PROXYL\text{-}(POG)_4POA(POG)_5]_3$:CBD complex, (C) $[PROXYL\text{-}(POG)_5POA(POG)_4]_3$:CBD complex and (D) $[PROXYL\text{-}(POG)_6POA(POG)_3]_3$:CBD complex, (E) $[(POG)_4POA(POG)_5C\text{-}PROXYL]_3$:CBD complex, (F) $[(POG)_4POA(POG)_5C\text{-carbamidomethyl}]_3$:CBD. The Gly^Ala mutation sites are highlighted. Figure 9G and 9H show two probable binding modes of [1 1PR0XYL-(P0G)$_3$PCG(P0G)$_4$]$_{3:}$:CBD complex.

Figure 10 is a set of plots showing HSQC NMR data obtained using the CBD - collagenous peptide interactions. Figure 10A is an overlay of $^1H\text{-}^{15}N$ HSQC spectrum of $[POGPO\text{-}^{15}N\text{-}G\text{-}(POG)_8]_3$ (black) with $^{1H}\text{-}^{15}N$ HSQC spectrum of $[POGPO\text{-}^{15}N\text{-}G\text{-}(POG)_8]_3$:CBD complex (red) at 1:1 ratio. Figure 10B shows an overlay of $^1H\text{-}^{15}N$ HSQC spectrum of $[POGPO\text{-}^{15}N\text{-}G\text{-}(POG)_2\text{-}POA\text{-}(POG)_5]_3$ (black) with $^1H\text{-}^{15}N$ HSQC spectrum of $[POGPO\text{-}^{15}N\text{-}G\text{-}(POG)_2JPOA\text{-}(POG)_5]_3$:CBD complex (red) at 1:1 ratio. Figure IOC shows an overlay of $^1H\text{-},^5N$ HSQC spectrum of $[(POG)_8\text{-}PO\text{-}^{15}N\text{-}G\text{-}POG]_3$ (black) with $^{1H}\text{-}^{15}N$ HSQC spectrum of $[(POG)_8\text{-}PO\text{-}^{15}N\text{-}G\text{-}POG]_3$:CBD complex (red) at 1:1 ratio. Figure 10D shows an

overlay of ^{1}H-^{15}N HSQC spectrum of $[(POG)_4$-POA-PO-^{15}N-G-POG$]_3$ (black) with ^{1}H-^{15}N HSQC spectrum of $[(POG)_4$-POA-PO-^{15}N-G-POG$]_3$:CBD complex (red) at 1:1 ratio.

Figure 11 shows the tissue distribution of S^{35} -PTH-CBD 1 hour and 12 hours after subcutaneous injection. Note the skin outline.

Figure 12 is a set of photographs documenting the hair growth on the back of mice at day 36 after depilation, treatment groups as indicated (Antagonist = PTH(7-33)-CBD, Agonist = PTH-CBD).

Figure 13 is a set of photographs showing the histology at Day 36 after the indicated treatment. Skin samples were taken from the dorsal region and processed for Hematoxylin and Eosin (H&E) staining. Representative sections are shown from each treatment group as indicated. (Antagonist = PTH(7-33)-CBD, Agonist = PTH-CBD).

Figure 14 is a graph showing the hair follicle counts per high powered field. Anagen VI hair follicles were counted by two independent observers in a blinded fashion. Results are expressed as mean +/- standard deviation. **=$p<0.01$ vs. no chemo ANOVA followed by Dunnett's test. (Antagonist = PTH(7-33)-CBD, Agonist = PTH-CBD).

Figure 15 is a set of photographs showing the hair growth on the back of the mice after each of the indicated treatments and a graph showing the results of a grey scale analysis of the hair at the injection site over time after the injection.

Figure 16 is a set of photographs showing the hair on the back of mice after the indicated treatment without prior depilation.

Figure 17 is a set of photographs and a graph showing the grey scale analysis of hair growth on the backs of mice comparing the indicated treatments with the PTH-CBD being administered prior to the chemotherapy as opposed to after chemotherapy began.

Figure 18 is a photograph of three mice 13 days after waxing to remove hair and treatment with PTH-CBD, PTH antagonist-CBD or vehicle alone.

Figure 19 is a set of photographs of mice showing hair regrowth in a model of alopecia areata after treatment with a control or with PTH-CBD.

Figure 20 is a graph showing the endogenous parathyroid hormone levels in ovarectomized aged rats injected with a single dose of human PTH-CBD 6 months prior to sacrifice.

DETAILED DESCRIPTION

Methods of delivering a therapeutic agent by administering a composition comprising a bacterial collagen-binding polypeptide segment linked to a therapeutic agent to a subject in need of treatment with the therapeutic agent are provided herein. In this embodiment, the therapeutic agent is not a PTH/PTHrP receptor agonist or antagonist and is not a bFGF or EGF polypeptide. The bacterial collagen-binding polypeptide segment delivers the therapeutic agent to sites of partially untwisted or under-twisted collagen.

In addition, methods of treating collagenopathies, such as osteogenesis imperfecta (01), by administering a composition comprising a bacterial collagen-binding polypeptide segment linked to a PTH/PTHrP receptor agonist to a subject in need of treatment for a collagenopathy are provided. Collagenopathies include but are not limited to osteogenesis imperfecta, Stickler's syndrome, Ehlers-Danlos syndrome, Alport's syndrome, Caffey's disease, and localized collagen or cartilage damage. Many of these diseases are caused by genetic defects that result in the collagen in certain tissues being under twisted or partially untwisted.

For example, individuals with OI carry a mutation which causes an amino acid change in collagen changing a glycine to a bulkier amino acid which results in disruption of the triple helix structure of the collagen and under-twisting of the collagen. In the Examples, we demonstrate that the bacterial collagen-binding polypeptides described herein target and bind to these areas of under-twisted collagen. Thus, use of the collagen-binding polypeptides described herein to deliver a therapeutic agent capable of treating 0 1to the sites of under-twisted collagen may allow more effective treatment.

The collagen-binding polypeptide segment and the therapeutic agent may be chemically cross-linked to each other or may be polypeptide portions of a fusion protein. The terms "fusion protein" and "fusion polypeptide" may be used to refer to a single polypeptide comprising two functional segments, e.g., a collagen-binding polypeptide segment and a polypeptide based therapeutic agent, such as PTH/PTHrP receptor agonist polypeptide segment. The fusion proteins may be any size, and the single polypeptide of the fusion protein may exist in a multimeric form in its functional state, e.g., by cysteine disulfide connection of two monomers of the single polypeptide. A polypeptide segment may be a synthetic polypeptide or a naturally occurring polypeptide. Such polypeptides may be a portion of a polypeptide or may comprise one or more mutations. The two polypeptide segments of the fusion proteins can be linked

directly or indirectly. For instance, the two segments may be linked directly through, e.g., a peptide bond or chemical cross-linking, or indirectly, through, e.g., a linker segment or linker polypeptide. The peptide linker may be any length and may include traditional or non-traditional amino acids. For example, the peptide linker may be 1-100 amino acids long, suitably it is 5, 10, 15, 20, 25 or more amino acids long such that the collagen binding portion of the fusion polypeptide can mediate collagen binding and the therapeutic agent can have its therapeutic effect. Peptide linkers may include but are not limited to a PKD (polycystic kidney disease) domain from a collagenase or other protein such as in SEQ ID NO: 2, a GST or His-tag, or a Ser or Gly linker.

The collagen-binding polypeptide segment is a polypeptide that binds collagen and may be part of a larger fusion protein, bioactive agent, or pharmaceutical agent. Determination of whether a composition, polypeptide segment, fusion protein, or pharmaceutical or bioactive agent binds collagen can be made as described in U.S. Patent Publication No. 2010/0129341, which is incorporated herein by reference in its entirety. Briefly, it is incubated with collagen in binding buffer, and the mixture is then filtered through a filter that would otherwise allow it to pass through but that blocks the collagen and therefore holds back materials that bind to the collagen. The filtrate is then assayed for the presence of the composition, polypeptide segment, fusion protein, or pharmaceutical or bioactive agent. Suitably, at least 80%, 85%, 90%, 95%, 98% or more suitably at least 99% of the collagen-binding composition, polypeptide segment, fusion protein, or pharmaceutical or bioactive agent is retained by the filter in this assay, as compared to when the filtration is performed without collagen.

The collagen-binding polypeptide segment may be a bacterial collagen-binding polypeptide segment. It may be a Clostridium collagen-binding polypeptide segment. The collagen-binding polypeptide segment may be a segment of a collagenase, or a bacterial collagenase, or a Clostridium collagenase. Suitably the polypeptide segment is only a portion of the collagenase and the collagen-binding polypeptide segment does not have collagenase activity. The collagen-binding polypeptide may be a bacterial M9B (including those derived from *Bacillus* spp. and *Clostridium* spp.) or M9A (including those derived from *Vibrio* spp.) collagen-binding protein or a collagen-binding peptide derived from such a protein. By "derived from" we mean that the peptide is a fragment of the full-length protein, a peptide that has amino acid changes relative to the wild-type protein or a combination thereof. The key is that the

peptide retains the ability to bind collagen. For example, a peptide may be derived from a protein by selecting a region of the protein capable of binding to collagen. Compositions including a bacterial collagenase as a collagen binding peptide are described in US Patent Publication No. 2010/0129341, which is hereby incorporated herein by reference in its entirety.

Figure 1 shows a sequence alignment of the collagen-binding region of several M9B bacterial collagen-binding proteins included as SEQ ID NOs: 13-34. As can be seen from the sequence alignment, these proteins have a relatively small amount of sequence identity (about 30%), but they all bind to collagen in a similar fashion and are believed to have similar conformation as discussed in the Examples. Thus any of the peptides shown in Figure 1 or collagen-binding fragments thereof can be used in the compositions and methods described herein. In Figure 1, the amino acid residues critical for the conformation of the peptide and for the collagen-binding activity are underlined and shown in green and blue respectively. The key amino acid residues for collagen-binding are a tyrosine or phenylalanine at position 970 of ColG, position 977 of the ColH sequence of SEQ ID NO: 1 (position 937 in Figure 1) or a similar position of one of the sequences shown in Figure 1; a tyrosine at position 994 of of ColG, position 1000 of the ColH sequence of SEQ ID NO: 1 (position 962 in Figure 1) or a similar position of one of the sequences shown in Figure 1; a tyrosine, phenylalanine or histidine at position 996 of ColG, position 1002 of the ColH sequence of SEQ ID NO:l (position 964 in Figure 1) or a similar position of one of the sequences shown in Figure 1. Thus a peptide with relatively low sequence identity, sharing the structure and function of the ColG protein may also be used as a collagen binding domain (CBD) herein.

In one embodiment, the collagenase is ColH, SEQ ID NO: 6. The collagen-binding polypeptide segment may be or may include residues 901-1021 of SEQ ID NO:6 (residues 34-158 of SEQ ID NO:l), or a fragment of residues 34-158 of SEQ ID NO:l at least 8, 10, 12, 15, 20, 25, 30, 40, 50, 60, 70 ,80, 90, 100, 110 or 120 amino acid residues in length. The collagen-binding polypeptide segment is at least *50%*, *60%*, *70%*, 80%o, or at least 85%, at least *90%*, at least 95%, at least 96%, at least 98%, or at least 99% identical to residues 34-158 of SEQ ID NO: 1. The collagen-binding polypeptide segment may be or may include residues 807-1021 of SEQ ID NO:6 (residues 37-25 1 of SEQ ID NO:2), or a fragment of residues 807-1021 of SEQ ID NO:6 at least 8, 10, 12, 15, 20, 25, 30, 40, 50, 60, 70 ,80, 90, 100, 110 or 120 amino acid residues in length. Residues 807-901 comprise the polycystic kidney disease (PKD) domain of

the collagen-binding protein. Those of skill in the art will appreciate that other linkers could be used to link the collagen-binding peptide to a therapeutic agent as outlined above. The collagen-binding polypeptide segment may be or may comprise a fragment of residues 901-1021 of SEQ ID NO:6, e.g., a fragment of at least 8, at least 10, at least 20, at least 30 at least 40, or at least 50 consecutive amino acid residues of residues 901-1021 of SEQ ID NO:6. Suitably the collagen-binding polypeptide consists of residues 894-1008, 894-1021, 901-1021, or 901-1008 of SEQ ID NO: 6 or a homolog thereof as shown by the sequence alignment in Figure 9.

Among other proteins the collagen-binding segment can be derived from are ColG (Matsushita et al, (1999) J. Bacteriol. 181 :923-933), a class I collagenase from *Clostridium histolyticum.* ColH is a class II collagenase (Yoshihara et al., (1994) J. Bacteriol. 176: 6489-6496). The collagen-binding polypeptide segment may also be a polypeptide segment from any one of the protein sequences provided in Figure 1 which aligns collagen-binding peptides from members of Clostridium and Bacillus. Those of skill in the art will appreciate that other members of this collagen-binding protein family may be useful in the methods described herein.

The therapeutic agents linked to the collagen-binding polypeptide may be any suitable pharmaceutical or other active agent, including but not limited to, osteogenic promoters, antimicrobials, anti-inflammatory agents, polypeptides such as recombinant proteins, cytokines or antibodies, small molecule chemicals or any combination thereof. Suitably the therapeutic agents are capable of promoting bone growth, decreasing inflammation, promoting collagen stability. Suitably, the therapeutic agent is one whose therapeutic effect is in the region of collagen or damaged collagen. The therapeutic agent may include, but is not limited to, bone morphogenic protein (BMP), G-CSF, FGF, BMP-2, BMP-3, FGF-2, FGF-4, anti-sclerostin antibody, growth hormone, IGF-1, VEGF, TGF-β, KGF, FGF-10, TGF-a, TGF-β1, TGF-β receptor, CT, GH, GM-CSF, EGF, PDGF, celiprolol, activins and connective tissue growth factors. In alternative embodiments, the active agent may be a PTH/PTHrP receptor agonist or antagonist.

Bone loss due to a collagenopathy such as osteogenesis imperfecta, Stickler's syndrome or others which put an individual at higher risk for a bone fracture due to a collagen defect could be treated by administration of a bone anabolic peptide. The CBD may target the bone anabolic agents to sites where the collagen is malformed and thus may prevent fracture.

Vascular fragility due to defects such as Ehlers-Danlos syndrome type IV, Alport's syndrome or other diseases where blood vessel rupture is more likely due to a defect in collagen formation may be administered peptides that stimulate vascular growth or repair. The CBD will target the peptide to the areas having collagen damage and these areas are likely to have damaged vessels. The therapeutic agents will stimulate growth and repair at the site of damage and prevent vessel rupture.

Skin fragility due to disorders such as Ehlers-Danlos syndrome, Caffey's disease or other diseases where weakening of the skin due to a collagen defect leads to hyperelasticity, easy bruising or poor wound healing. Dermal and epidermal growth factors may serve as therapeutic agents which when linked to CBD and delivered to areas of damaged collagen will stimulate growth and repair of the skin, preventin striae and improving healing.

Collagen defects may also lead to cartilage malformation or insufficiency. Cartilage growth factors could be delivered locally to sites of damaged cartilage to aid in repair and restore function.

The PTH/PTHrP receptor agonist polypeptide segment may be a synthetic polypeptide or a naturally occurring polypeptide. Such polypeptides may be a portion of a polypeptide or may comprise one or more mutations. The mutations may make the PTH/PTHrP receptor agonist a better or worse agonist as compared to the wild-type PTH/PTHrP. Agonist activity with the PTH/PTHrP receptor can be assayed as described in Example 3 below by a cAMP stimulation assay. An agonist will stimulate cAMP synthesis in the assay described. Suitably, an agonist can activate receptor activity at least 10%, 20%, 30%, 40%, 50%, 60%, 70%, 80%, 90%, 100% or even 110% or 120% as much as wild-type PTH(l-34).

The PTH/PTHrP receptor agonist polypeptide segment is a PTH or PTHrP polypeptide segment. One human isoform of PTH is SEQ ID NO:7. One human isoform of PTHrP is SEQ ID NO: 8. While the human isoforms are provided, those of skill in the art will appreciate that other non-human-derived isoforms may be used as well. Such non-human-derived isoforms may be able to interact with human PTH/PTHrP receptor and vice versa. The PTH/PTHrP receptor agonist polypeptide segment may be or may include residues 1-33 of SEQ ID NO:l (residues 1-33 of PTH (SEQ ID NO: 7)). The PTH/PTHrP receptor agonist polypeptide segment may be or

may include residues 1-34 of PTH (SEQ ID NO:7). In other embodiments, it is a fragment of residues 1-34 of PTH (SEQ ID NO:7). In other embodiments, the PTH/PTHrP receptor agonist polypeptide segment may be or may include residues 1-84 of PTH (SEQ ID NO:7). In other embodiments, the PTH/PTHrP receptor agonist polypeptide segment may be or may include residues 1-14 of PTH (SEQ ID NO:7). In still other embodiments, the PTH/PTHrP receptor agonist is a PTH or PTHrP polypeptide segment for any other species.

The PTH/PTHrP receptor antagonist can include in one embodiment PTH(7-34), i.e., residues 7-34 of PTH (SEQ ID NO:7). In another embodiment, it is or includes residues 7-33 of PTH (SEQ ID NO:7). In other embodiments, it is a fragment of residues 7-34 of SEQ ID NO: 8. In another embodiment, the PTH/PTHrP receptor antagonist includes PTH(7-14), i.e., residues 7-14 of PTH (SEQ ID NO:7). In another embodiment, the PTH/PTHrP receptor antagonists include ((-l)-33) of PTH/PTHrP. In another embodiment, the PTH/PTHrP receptor antagonists include residues 1-14 of PTH with an N-terminal extension. Adding an N-terminal extension to PTH or active N-terminal fragments of PTH converts the PTH peptides to antagonists. The N-terminal extension can be 1, 2, 3, 4, 5, or more amino acids in length. The identity of the amino acids in the N-terminal extension is typically not important. In one embodiment, the PTH/PTHrP receptor antagonist includes residues 1-33 of PTH with a Gly-Ser extension at the N-terminus (SEQ ID NO:l 1). In another embodiment, the PTH/PTHrP receptor antagonist includes PTHrP(7-34), i.e., residues 7-34 of SEQ ID NO:8, or a fragment of residues 7-34 of SEQ ID NO: 8. In another embodiment, the PTH/PTHrP receptor antagonist includes mouse TIP(7-39) (See Hoare S R, Usdin T B. 2002. Specificity and stability of a new PTH1 receptor antagonist, mouse TIP(7-39). Peptides 23:989-98.). Other PTH/PTHrP receptor antagonists that may be used in the fusion proteins are also disclosed in Hoare et al. The PTH/PTHrP receptor antagonist may be a fragment of at least 8, 10, 12 or more amino acids from residues 1-34 of SEQ ID NO:7. In other embodiments the PTH/PTHrP receptor antagonist may be PTH/PTHrP receptor antagonist polypeptide from another species.

In one embodiment, the therapeutic agent or PTH/PTHrP receptor agonist or antagonist polypeptide segment is N terminal to the collagen-binding polypeptide segment in the fusion protein. That is, the two polypeptide segments each have an N-terminal and a C-terminal, and the N-terminal of the collagen-binding polypeptide segment is linked directly or indirectly, e.g.,

through a linker polypeptide segment (such as PKD, a Glycine or Serine linker) to the C-terminal of the therapeutic agent or PTH/PTHrP agonist or antagonist polypeptide segment.

The fusion proteins described above comprising (a) a collagen-binding polypeptide segment linked to (b) a therapeutic agent or a PTH/PTHrP receptor agonist or antagonist polypeptide segment can be replaced by pharmaceutical agents comprising (a) a collagen-binding polypeptide segment linked to (b) a therapeutic agent or PTH/PTHrP receptor agonist or a non-peptidyl PTH/PTHrP receptor agonist. An example of a non-peptidyl PTH/PTHrP receptor agonist is compound AH3960 (Rickard et al, (2007) Bone 39:1361-1372).

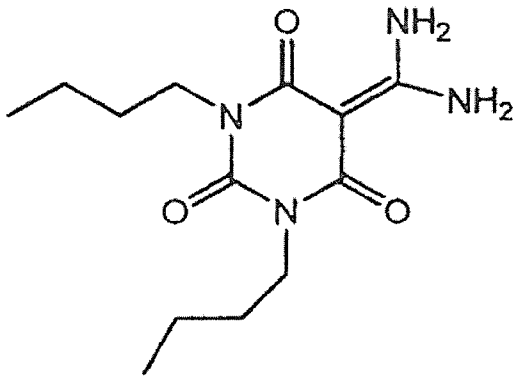

AH3960

AH3960 contains two amino groups. Amino groups in small chemical molecules such as AH3960 can be used to cross-link the therapeutic agent to amino groups on the collagen-binding polypeptide segment through a cross-linker such as DSG (disuccinimidyl glutarate) or through the combination of SANH (succinimidyl-4-hydrazinonicotinate acetone hydrazone) and SFB (succinimidyl-4-formyl benzoate). Therapeutic agents can be cross-linked through their amino group to a carboxyl group of the collagen-binding polypeptide segment by EDC (l-ethyl-3-[3-dimethylaminopropyljcarbodiimide hydrochloride) or vice versa. These cross-linking products are available from Pierce (piercenet.com, Thermo Fisher Scientific Inc., Rockford, 111.). Protocols and reaction conditions are also available in the product literature from Pierce (piercenet.com).

In another embodiment of the pharmaceutical agents comprising (a) a collagen-binding polypeptide segment; linked to (b) a polypeptide therapeutic agent or a PTH/PTHrP receptor agonist or antagonist polypeptide segment, segment (a) and segment (b) are separate polypeptides, and the two polypeptides are linked by chemical cross-linking. The two

polypeptides can be cross-linked through amino groups by reagents including DSG (disuccinimidyl glutarate) or glutaraldehyde. They can also be cross-linked through amino groups by derivatizing one polypeptide with SANH (succinimidyl-4-hydrazinonicotinate acetone hydrazone) and the other with SFB (succinimidyl-4-formyl benzoate), and then mixing the two derivatized polypeptides to cross-link. The two polypeptides can be cross-linked between an amino group of one polypeptide and a carboxyl of the other by reaction with EDC (l-ethyl-3-[3-dimethylaminopropyl]carbodiimide hydrochloride). The polypeptides can also be cross-linked (e.g., covalently coupled) by any other suitable method known to a person of ordinary skill in the art. These cross-linking reagents are available from Pierce (piercenet.com, Thermo Fisher Scientific Inc., Rockford, 111.). Protocols and reaction conditions are also available in the product literature from Pierce (piercenet.com). These and other applicable cross-linking methods are described in U.S. published patent applications 2006/0258569 and 2007/02241 19.

Also provided herein are methods of treating hyperparathyroidism by administering PTH-CBD to a subject in need of treatment for hyperparathyroidism. In one embodiment the PTH administered to the subject may be a PTH from a different species. As shown in the Examples a single administration of CBD-PTH to ovarectomized aged rats was able to reduce the amount of endogenous PTH produced by the animal. Thus, administration of PTH-CBD to individuals suffering from hyperparathyroidism may experience a decrease in symptoms associated with hyperparathyroidism and have decreased levels of PTH after administration of PTH-CBD.

The effects of PTH agonists and antagonists on hair growth have been studied for over almost 15 years. PTH has a common receptor with PTH-related peptide (PTHrP), which is normally produced by dermal fibroblasts. PTHrP affects keratinocyte proliferation/differentiation and modulates the hair cycle. Most of the testing on hair growth effects has been performed with PTH antagonists, as indications from initial testing were that these were the most effective agents. Both injected and topical formulations have been tested in animal models of chemotherapy-induced alopecia and in the SKH-1 hairless mouse. Part of the effect of PTH antagonists on hair growth is to transition the hair follicles into a dystrophic catagen stage, which protects them from chemotherapeutic damage. However, clinical trials of topical PTH antagonists for chemotherapy-induced alopecia by IGI Pharmaceuticals were discontinued in phase 2 because of limited efficacy. Thus new compositions for treating alopecia are needed.

The problems of delivery and retention of PTH to the skin can be overcome by using collagen-targeted PTH analogs. To accomplish this, we synthesized several fusion proteins of different PTH agonists and antagonists linked to a collagen binding domain derived from the ColHl collagenase of *Clostridium histolyticum*. In the studies described in the Examples, we found that the agonist compound PTH-CBD promotes transition of hair follicles to the anagen phase and has potent effects on hair growth. The antagonist compound PTH(7-33)-CBD had little effect on hair growth in chemotherapy models and had a deleterious effect on hair regrowth after depilation. Compounds such as PTH-CBD, which promote anagen phase transition of hair follicles, have been sought after due to their potential to treat a large variety of disorders of hair loss. PTH-CBD appears to have a similar mechanism of action to cyclosporine, which also promotes transition of hair follicles to anagen phase, although the mechanism is less likely to be the result of direct effects on WNT signaling. While clinical use of cyclosporine for this purpose is limited by systemic toxicity, PTH-CBD has not shown toxic effects, even with systemic administration.

Thus in another aspect, methods of increasing hair growth are provided herein. The methods include administering a CBD linked to a PTH/PTHrP receptor agonist to a subject in need of treatment to induce hair growth or stop hair loss. The method is applicable to individuals with alopecia, including chemotherapy induced alopecia, but also alopecia areata, alopecia caused by male pattern baldness, polycystic ovarian syndrome or other hair loss. The compositions may be administered locally or topically to treat hair loss.

In another aspect, methods of slowing hair growth or regrowth after a hair removal procedure by administering a CBD linked to a PTH/PTHrP receptor antagonist to a subject are provided. In one embodiment, the PTH antagonist composition is applied locally, topically. The PTH antagonist may be applied after a hair removal procedure to prevent or slow hair regrowth. As described in the Examples, we have demonstrated that hair regrowth is slowed after waxing in animals treated with CBD-PTH antagonist as compared to control animals treated with PTH-CBD or vehicle alone. The compositions may be administered locally or topically to block hair growth.

The compositions described herein may be administered by any means known to those skilled in the art, including, but not limited to, oral, topical, intranasal, intraperitoneal, parenteral, intravenous, intramuscular, intradermal or subcutaneous. Thus the compositions may be

formulated as an ingestable, injectable, topical or suppository formulation. The composition may be formulated for administration by injection to result in systemic administration or local administration. The compositions may also be delivered with in a liposomal or time-release vehicle. The compositions may also be delivered in a site-directed delivery vehicle, such as but not limited to, a targeted liposome or an absorbable collagen sponge carrier or other implant.

The inventors have found that when administering compositions including a CBD subcutaneously it binds locally at the site of injection if the composition is dissolved in neutral pH buffer. But if the composition is dissolved in a low pH buffer, for example a buffer having pH 5.0 or pH 4.5 or below, the collagen-binding domain does not bind collagen, and the composition has time to disperse systemically before it binds collagen elsewhere in the body at neutral pH. Thus systemic administration of the compositions involves administering the composition dissolved in buffer or aqueous solution at a pH lower than about 5.0 or at pH 4.5 or below. In another embodiment, systemic administration of the compositions involves administering the fusion proteins dissolved in aqueous solution at pH lower than about 6.0. Alternatively, if the skin condition is localized, the compositions described herein may be administered in a buffer with a pH of 6.0, 6.5, 7.0, 7.5 or above in order to allow for localized delivery of the compositions to the affected area of the skin.

Pharmaceutical compositions for topical administration may also be formulated using methods and compositions such as those available to those skilled in the art. For example, gels, creams or liposome preparations may be suitable for topical delivery. These delivery vehicles may be formulated to mediate delivery to the lower layers of the skin or to allow for extended release of the pharmaceutical at the site of application.

The compositions can be administered as a single dose or as divided doses. For example, the composition may be administered two or more times separated by 4 hours, 6 hours, 8 hours, 12 hours, a day, two days, three days, four days, one week, two weeks, or by three or more weeks. Optionally, such treatment may be repeated, for example, every 1, 2, 3, 4, 5, 6, or 7 days, or every 1, 2, 3, 4, and 5 weeks or every 1, 2, 3, 4, 5, 6, 7, 8, 9, 10, 11, or 12 months. The composition is expected to be more effective than a comparable or control composition comprising the therapeutic agent or a PTH/PTHrP receptor agonist that is not linked to a collagen-binding protein. In one embodiment, a smaller amount of the composition may be used or the composition may be administered less frequently than a comparable composition

comprising the therapeutic agent or a PTH/PTHrP receptor agonist which is not linked to a collagen-binding protein.

The dosage amounts and frequencies of administration provided herein are encompassed by the terms therapeutically effective and prophylactically effective. The individual doses of pharmaceutical agents comprising a collagen-binding polypeptide segment linked to a therapeutic agent may be approximately the same on a molar basis as doses used for the therapeutic agent alone. It is expected that the pharmaceutical agents comprising a collagen-binding polypeptide segment linked to a therapeutic agent may be administered less frequently, because linking the agent to the collagen-binding polypeptide segment gives it much more prolonged activity *in vivo.*

Administration of the compositions to a subject in accordance with the invention appears to exhibit beneficial effects in a dose-dependent manner. Thus, within broad limits, administration of larger quantities of the compositions is expected to achieve increased beneficial biological effects than administration of a smaller amount. Moreover, efficacy is also contemplated at dosages below the level at which toxicity is seen.

It will be appreciated that the specific dosage administered in any given case will be adjusted in accordance with the compositions being administered, the disease to be treated or inhibited, the condition of the subject, and other relevant medical factors that may modify the activity of the agent or the response of the subject, as is well known by those skilled in the art. For example, the specific dose for a particular subject depends on age, body weight, general state of health, diet, the timing and mode of administration, the rate of excretion, medicaments used in combination and the severity of the particular disorder to which the therapy is applied. Dosages for a given patient can be determined using conventional considerations, e.g., by customary comparison of the differential activities of the compositions of the invention and of the therapeutic agent administered alone, such as by means of an appropriate conventional pharmacological or prophylactic protocol.

The maximal dosage for a subject is the highest dosage that does not cause undesirable or intolerable side effects. The number of variables in regard to an individual prophylactic or treatment regimen is large, and a considerable range of doses is expected. The route of administration will also impact the dosage requirements. It is anticipated that dosages of the compositions will reduce symptoms of the condition being treated by at least 10%, 20%, 30%o,

40%, 50%, 60%, 70%, 80%, *90%* or 100% compared to pre-treatment symptoms or symptoms is left untreated. It is specifically contemplated that pharmaceutical preparations and compositions may palliate or alleviate symptoms of the disease without providing a cure, or, in some embodiments, may be used to cure the disease or disorder.

Suitable effective dosage amounts for administering the compositions may be determined by those of skill in the art, but typically range from about 1 microgram to about 10,000 micrograms per kilogram of body weight weekly, although they are typically about 1,000 micrograms or less per kilogram of body weight weekly. In some embodiments, the effective dosage amount ranges from about 10 to about 10,000 micrograms per kilogram of body weight weekly. In another embodiment, the effective dosage amount ranges from about 50 to about 5,000 micrograms per kilogram of body weight weekly. In another embodiment, the effective dosage amount ranges from about 75 to about 1,000 micrograms per kilogram of body weight weekly. The effective dosage amounts described herein refer to total amounts administered, that is, if more than one compound is administered, the effective dosage amounts correspond to the total amount administered.

The effectiveness of the compositions described herein may be enhanced by at least 10%, at least 15%, at least 20%, at least 25%, at least 30%, at least 35%, at least 40%, at least 45%, at least 50%, at least 55%, at least 60%, at least 65%, at least 70%, at least 75%, at least 80%, at least 85%, at least 90%, at least 95%, or at least 100% relative to a control treated with the therapeutic agent alone. It will be appreciated that the effectiveness of the treatment in any given case will be enhanced variably in accordance with the specific compositions used, the type of disease being treated, the condition of the subject, the specific formulations of the compounds and other relevant medical factors that may modify the activity of the compositions or the responses of the subject as is appreciated by those of skill in the art.

The following examples are meant only to be illustrative and are not meant as limitations on the scope of the invention or of the appended claims. All references cited herein are hereby incorporated by reference in their entireties.

EXAMPLES

Example 1: CBD targets partially untwisted or uintertwisted regions of collagen

Clostridium histolyticum collagenase causes extensive degradation of collagen in the connective tissue resulting in gas gangrene. The C-terminal collagen-binding domain (CBD) of these enzymes is the minimal segment required to bind to the collagen fibril. CBD binds unidirectionally to the partially untwisted C-terminus of triple helical collagen. Whether CBD could also target under-twisted regions even in the middle of the collagen triple helix was examined. Partially untwisted collageneous peptides were synthesized by introducing a Gly^Ala substitutions into the collagen **$[(POG)_xPOA(POG)_y]_3$** where x+y=9 and χ>3). ^{1}H-^{15}N heteronuclear single quantum coherence nuclear magnetic resonance (HSQC NMR) titration studies with ^{15}N-labeled CBD demonstrated that the untwisted mini-collagen binds to a 10 A wide 25 A long cleft. Six untwisted collagenous peptides each labeled with a nitroxide radical were then titrated with ^{15}N-labeled CBD. The paramagnetic nuclear spin relaxation effects showed that CBD binds close to either the Gly^Ala substitution site or to the C-terminus of each mini-collagen. Small angle X-ray scattering (SAXS) measurements revealed that CBD prefers to bind the Gly->Ala site rather than the C-terminus. The HSQC NMR spectra of ^{15}N-labeled mini-collagen and untwisted mini-collagen were unaffected by the titration of unlabeled CBD. The results imply that CBD binds to the partially unwound region of the mini-collagen but does not actively unwind the triple helix.

Materials and Methods:

^{15}N-labeled protein production: The s3b (Gly893-Lysl008) peptide derived from *Clostridium histolyticum* class I collagenase (ColG) was expressed as a glutathione S-transferase (GST)-fusion protein. The GST-tag was cleaved off by thrombin, and CBD was purified as described previously. Matsushita, et al, (2001) *J Biol Chem* 276, 8761-8770. Uniform ^{15}N isotope labeling was achieved using Tanaka minimal medium containing 40 mM $^{15}NH_4C1$. The labeling efficiency was estimated to be 99.6% by matrix-assisted laser desorption/ionization-time of flight mass spectrometry (MALDI-TOF-MS).

Peptides: (POG)io (SEQ ID NO: 35) was purchased from Peptide Institute, Inc. (Osaka, Japan). Other peptides were constructed by a standard N-(9-fluorenyl) methoxycarbonyl (Fmoc)-based strategy on Rink-amide resins (Novabiochem, Darmstadt, Germany). N-terminal

spin-labeling was performed on the resin by the treatment with 5 equivalents of 3-carboxy-PROXYL (Aldrich), 1-hydroxybenzotriazole, diisopropylcarbodiimide in N,N-dimethylformamide at room temperature for 2 hours. Peptide cleavage and de-protection steps were performed by a treatment with a standard trifluoroacetic acid (TFA) scavenger cocktail (TFA: w-cresol: thioanisole: water: triisopropylsilane = 82.5: 5: 5: 5: 2.5, v/v). The spin-labeling at Cys residues was performed using 3-(2-iodoacetamido)-PROXYL (IPSL, Sigma-Aldrich). Briefly, 10 molar excess of IPSL dissolved in ethanol was added to the same volume of 10 mg/ml peptide in 0.1 M Tris-HCl (pH 8.8), 5 mM ethylenediaminetetraacetic acid. After reacting at room temperature for 1 hr, the reaction was quenched by adding excess dithiothreitol. All peptides were purified by reverse-phase HPLC using a Cosmosil 5Ci$_8$ AR-II column (Nacalai Tesque, Kyoto, Japan) and characterized by MALDI-TOF-MS. All the measured masses agreed with the expected values. The chemical structures of synthesized peptides are shown in Fig. 2.

Circular dichroism spectroscopy: The triple helical conformation and the stability of the collagenous peptides were verified using CD spectroscopy (See Fig. 3 and 4). CD spectra were recorded with a J-820 CD spectropolarimeter (JASCO Co., Hachioji, Japan) equipped with a Peltier thermo controller, using a 0.5-mm quartz cuvette and connected to a data station for signal averaging. All peptide samples were dissolved in water (1 mg/ml), and stored at 4 °C for 24 h. The spectra are reported in terms of ellipticity units per mole of peptide residues $[9]_{mrw}$. Thermostability of the triple helix was monitored by the $[\theta]_{225}$ values of each peptide with increasing temperature at the rate of 0.3 °C/min.

NMR spectroscopy: NMR experiments were performed on a Bruker 700 MHz spectrometer equipped with cryoprobe™. All the NMR titration experiments were carried out at 16 ± 0.5 °C. The working temperature is lower than the melting temperatures (T_M) of all the paramagnetic spin-labeled collagenous peptides (Table 1) used. The concentration of the protein was 0.1 mM in 50 mM Tris-HCl (pH 7.5) containing 100 mM NaCl and 20 mM $CaCl_2$. The dilution effect on the course of titration was minimized by the titration of a highly concentrated (4 mM) peptide stock. Aliquots of collagenous peptide were added to the protein and equilibrated for 5 min before acquiring ^{1}H-^{15}N HSQC spectra. The pH of the NMR samples monitored during the titration exhibited no significant shift in the pH (within ± 0.2 units).

Table 1: Melting temperatures *(T_m)* of various mini-collagen peptides that were used in NMR titration and the experiments described herein.

Peptides	Tm (° C)	SEQ ID NO:
$(POG)_4POA(POG)_5$	29	38
PROXYL-$(POG)_4POA(POG)_5$	29	38
PROXYL-$(POG)_3POA(POG)_6$	28	39
PROXYL-$(POG)_5POA(POG)_4$	28	37
PROXYL-$(POG)_6POA(POG)_3$	27	36
$(POG)_4POA(POG)_5$C-PROXYL	30	41
^{11}PROXYL-$(POG)_3PCG(POG)_4$	28	40

Dynamic light scattering experiments: The dynamic light scattering (DLS) data were collected using DynaPro-E equipped with a temperature controlled microsampler on the samples of CBD, collagenous peptides and CBD:mini-collagen complexes in 10 mM Tris-HCl (pH 7.5) containing 100 mM sodium chloride and 20 mM $CaCl_2$. The protein samples were spun at 10,000 rpm for 10 min and were filtered through 0.02 μτη Whatman syringe directly into a 50-μL quartz cuvette. For each experiment, 20 measurements were made. The mean hydrodynamic radius *(RH),* standard deviation, polydispersity, and percent of peak area were analyzed using Dynamics V6 (Protein Solutions). The hydrodynamic radius and molecular weight estimations were calculated from time dependent fluctuations induced by Brownian motion as described. Proteau, et al. (2010) *Curr Protoc Protein Sci* Chapter 17, Unit 17 10.

Small angle X-ray solution scattering experiments: The small angle X-ray solution scattering (SAXS) data were collected on solutions of CBD, collagenous peptides and CBD-mini-collagen complexes in 10 mM Tris-HCl (pH 7.5), 100 mM NaCl and 20 mM $CaCl_2$ at SAXS/WAXS setup located at the 5-ID-D beamline of the DND-CAT synchrotron research center, Advanced Photon Source, Argonne National Laboratory (Argonne, IL). The main advantage of X-ray scattering is that it can be carried out in solution in near physiological conditions. Petoukhov et al., (2007) *Curr Opin Struct Biol* 17, 562-571. 1.2398 A (lOkeV) radiation was selected from the APS Undulator A insertion device using a Si-111 monochromator, with 1:1 horizontal focusing and higher harmonic rejection from a Rh coated mirror, and beam defining slits set at 0.3mm vertical by 0.25mm horizontal. A 1.6mm diameter capillary flow-cell with a flow rate of 4μl/sec was used to collect four frames with 10 second exposure time. The SAXS detector used was a Marl 65 scintillator fiber-optic coupled CCD detector and covered the momentum transfer range $0.005<¾<0.198$ A^{-1}, where $\boldsymbol{q} = 4\pi$ sinO/λ (2Θ

is the scattering angle). The WAXS detector was a custom Roper scintillator fiber-optic coupled CCD detector and covered 0.191<¾r<1.8 A $^{-1}$ S. Weigand, et al. (2009) *Advances in X-ray Analysis* 52, 58-68.

All scattering data were acquired at sample temperature of 10 °C. The four scattering patterns from each detector were averaged and merged with the rejection of outlying scans. For further analysis the program IGOR Pro 5.5 A (WaveMetrics) was used. The scattering profiles of the protein, peptide and their complexes were obtained after subtracting the buffer profiles. The reduced scattering data were plotted as scattering intensity *I(Q)* vs. *Q* (Fig. 4A). The radius of gyration, R_g, was obtained from the Guinier approximation by linear least squares fitting in the QR_g < 1 region, where the forward scattering intensity *1(0)* is proportional to the molecular weight of the protein complex. An indirect Fourier transformation of *I(Q)* data using GNOM provided the particle distribution function *P(r)* in the real space (Fig. 4B). Svergun, D. (1992) *J Appl Crystallogr* 25, 495-503. Where *P(r)* intersects with x-axis represents the maximum diameter D_{max} averaged in all orientations. The molecular envelopes were constructed for all the samples based on the SAXS data after *ab initio* calculation with the program GASBOR. Svergun, et al. (2001) *Biophys J* 80, 2946-2953. Simulated annealing minimization of randomly distributed dummy atoms converged to the protein structure after being tested for the best fit to the *I(Q)* scattering data. No symmetry restraints were applied to any of the shape reconstructions. For each of the complexes, ten *ab initio* models were calculated with GASBOR and averaged using DAMAVER. Svergun, D. (2003) *J Appl Crystallog* 36. The atomic models represented as a compact interconnected configuration of beads with diameter D_{max} were adjusted to fit the experimental data $I_{exp}(s)$ to minimize error. Atomic models were docked into *ab initio* envelopes with the program SUBCOMB. Kozin, M. B., and Svergun, D. (2000) *J Appl Crystallogr* 33, 775-777.

Docking model: The CBD-collagenous peptide complex is generated from Protein Data Bank entries of ColG s3b (INQD) and partially untwisted collagenous peptide ICAG (Ala mutation in 15th position). Other untwisted mini collagen molecules were generated by modifying ICAG using fragments derived from **[(POG)io]$_3$** structure (1K6F). To obtain the complex, the soft docking algorithm BiGGER was used. Palma, et al. (2000) *Proteins* 39, 372-384. Solutions were filtered using NMR titration data and the highest scoring model that

satisfied NMR and SAXS results was chosen. The manual adjustments were aided by the use of MIFit. McRee. (1999) *J Struct Biol* 125, 156-165.

Results and Discussion:

^{1}H-^{15}N HSQC NMR titration-CBD targeting the under-twisted sites in collagen: The untwisted collagenous peptide [(POG)$_6$POA(POG)$_3$]$_3$ (SEQ ID NO: 36) that has Ala in the 21st position from the N-terminus was synthesized. This peptide was further modified to accommodate a paramagnetic spin label at the N-terminus. ^{1}H-^{15}N HSQC NMR titrations were performed with [PROXYL-(POG)$_6$POA(POG)$_3$]$_3$ (SEQ ID NO: 36) and ^{15}N-labeled CBD at ratios ranging from 0.02:1 to 1.5:1. As demonstrated earlier, a total of eleven residues on the collagen binding interface (S928, W956, **G971,** K995, Y996, L924, T957, Q972, D974, L991 and V993) either disappeared from the HSQC spectrum or exhibited significant chemical shift perturbation from their original position on the course of titration. Philominathan,et al. (2009) *J Biol Chem* 284, 10868-10876. The PROXYL group on the N-terminus of the collagenous peptides can cause a distance-dependent line broadening of the NMR signals of CBD during the course of titration. In addition to the eleven residues, three more residues, V973, G975 and S979 exhibited appreciable line broadening and these residues eventually disappeared from the ^{1}H-^{15}N HSQC spectrum of CBD (Fig. 5A and 5B). When the [PROXYL-(POG)$_6$POA(POG)$_3$]$_3$(SEQ ID NO: 36):CBD complex was reduced with ascorbic acid those three residues reappeared in the ^{1}H-^{15}N HSQC spectrum. The disappearance of these three residues was consistent with the titration of [PROXYL-G(POG)$_7$]$_3$ (SEQ ID NO: 42) (C-terminus is at 22nd position from the N-terminal PROXYL) in our earlier publication. The comparison of the two titration results demonstrates that CBD is targeting the Gly→Ala substituted site. If CBD had only bound to the C-terminus of [PROXYL-(POG)$_6$POA(POG)$_3$]$_3$ (SEQ ID NO: 36) (C-terminus is at 30th position from the N-terminal PROXYL), we would expect to observe the disappearance of only one residue (V973) at the most, as in the published titration of [PROXYL-G(POG)$_7$(PRG)]$_3$(SEQ ID NO: 43). The disappearance of the residues (V973, G975 and S979) located at distal side from the Ca^{2+} binding site (Fig. 5C) confirmed that CBD binds unidirectionally to untwisted collagen as well. The collagen binding surface in CBD is a 10-A-wide and 25-A-long cleft. The width of the binding cleft in CBD matches the diameter of the triple helix and its length could accommodate

$[(POG)_3]_3$ (SEQ ID NO: 44). NMR results imply that CBD is binding to the under-twisted $[(POG)_2POA]_3$ (SEQ ID NO: 45) region of the collagen.

As paramagnetic relaxation enhancement is a distance dependent phenomenon, Gly->Ala substitution made at closer to the N-terminal PROXYL group should result in the disappearance of more residues on CBD. PROXYL containing collagenous peptides, [PROXYL-$(POG)_5POA(POG)_4]_3$ (SEQ ID NO: 37) (Ala at 18^{th} position from the N-terminal PROXYL), [PROXYL-$(POG)_4POA(POG)_5]_3$ (SEQ ID NO: 38) (Ala at the 15^{th} position from the PROXYL) and [PROXYL-$(POG)_3POA(POG)_6]_3$ (SEQ ID NO: 39) (Ala at the 12^{th} position from the PROXYL) were synthesized. Just as in the previous titrations, the line broadening effects on the residues of CBD were analyzed from the changes in the ^{1}H-^{15}N HSQC spectrum. The shorter the distance between Gly->Ala substitution site and the N-terminal PROXYL, more residues in CBD disappeared (Fig. 6 and Table 2). The magnitude of intensity drop for four amide resonances (Q972, G975, S979 and L924) of four different mini-collagen molecules was also the function of the distance (Fig. 7). The NMR results are consistent with CBD binding to the $[(POG)_2POA]3$ (SEQ ID NO: 45) region in each of the four under-twisted mini-collagen. The binding constants obtained from all the NMR titrations were <100μM indicating a moderate binding affinity between CBD and under-twisted mini-collagen.

Table 2: Residues that disappear due to the presence of PROXYL either at the N-terminus, C- terminus or in the middle of the collagenous peptide sequence.

No.	Peptides	Alanine position	Residues disappeared due to PROXYL
	Blank		
1	[(POG)10]3 (SEQ ID NO: 35)		
	PROXYL at N-terminus		
2	[PROXYL-(POG)6POA(POG)3]3 (SEQ ID NO: 36)	21	V973, G975, S979
3	[PROXYL-(POG)5POA(POG)4]3 (SEQ ID NO: 37)	18	Q972, V973, G975, S979
4	[PROXYL-(POG)4POA(POG)5]3 (SEQ ID NO: 38)	15	L946, Q972, V973, G975, S979
5	[PROXYL-(POG)3POA(POG)6]3 (SEQ ID NO: 39)	12	L946, G953, Q972, V973, D974, G975, N976, V978, S979
			S906, R929, S997, G998
	PROXYL at C-terminus		
6	[(POG)4POA(POG)5-PROXYL]3 (SEQ ID NO: 41)	15	V973, G975, S979 and S906, R929, S997, G998
	PROXYL in the middle		
7	[11PROXYL-(POG)3PCG(POG)4]3 (SEQ ID NO: 40)		

The helical conformation in both the $[(POG)_2POA]_3$ (SEQ ID NO: 45) and the C-terminal $[(POG)_3]_3$ (SEQ ID NO: 44) are similarly under-wound. The degree of rotation about the screw axis symmetry that describes the internal triple helical twist is defined as the helical twist value κ. The κ-value oscillates around an average value of -103° for $[(POG)io]_3$ (SEQ ID NO: 35). Bella (2010) *J Struct Biol* 170, 377-391. The C-terminus of a mini-collagen is under-twisted (κ value shifts from -103° to -110°) but the N-terminus is usually over-twisted. Collagen peptides with Gly->Ala substitution in the center of the peptide sequence still form triple helices, but with an abrupt under-twisting (κ value shifts from -103° to -115°) at the substitution site followed over-twisting to the norm. Because the $[(POG)_2POA]_3$ (SEQ ID NO: 45) region is somewhat more under-twisted than C-terminal $[(POG)_3]_3$ (SEQ ID NO: 44), the former could be preferentially targeted by CBD than the latter. However, CBD could still bind to the C-terminus.

CBD also targets the C-terminus of the under-twisted mini-collagen: To demonstrate that CBD binds to the C-terminal $(POG)_3$ (SEQ ID NO: 44) as well, a collagenous peptide $[(POG)_4POA(POG)_5\text{-PROXYL}]_3$ (SEQ **ID** NO: 38) was synthesized. $[(POG)_4POA(POG)_5$C-

PROXYL]$_3$ (SEQ ID NO: 41) was titrated with ^{15}N-labeled CBD at ratios 0.02:1 to 1.5:1 with increments of 0.02, and the changes in the HSQC spectrum of CBD were monitored. When the mini-collagen was bound to the cleft, a total of eleven residues on the collagen binding interface either line broadened or showed significant chemical shift perturbation as described earlier. Philominathan,et al. (2009) *J Biol Chem* 284, 10868-10876. Four additional residues S906, R929, S997 and G998 disappeared from the HSQC spectrum due to PROXYL (Figs. 6 A, B and D). These peaks reappeared upon addition of ascorbic acid. This phenomenon is identical to our previous titration of [GPRG(POG)$_7$C-PROXYL]$_3$ (SEQ ID NO: 46) when CBD bound the C-terminus. If CBD were to bind only to the partially unwound Ala site, we would have observed the disappearance of fewer residues. Thus in addition to targeting the (POG)$_2$POA (SEQ ID NO: 45) region of the collagenous peptide, CBD also binds to the C-terminal (POG)$_3$ (SEQ ID NO: 44). As described, the helical confirmation of both the (POG)$_2$POA (SEQ ID NO: 45) region and the C-terminal (POG)$_3$ (SEQ ID NO: 44) are similarly under-twisted compared to the norm. Bella. (2010) *J Struct Biol* 170, 377-391. Our current explanation for why CBD is targeting the under-twisted regions is that the partial unwinding positions main-chain carbonyl groups to favor hydrogen-bonding interactions with the hydroxyl group of Tyr994. Tyr994 mutation to Phe resulted in 12-fold reduction in binding to mini-collagen, and the mutation to Ala lost binding capability. Wilson, et al. (2003) *EMBO J22*, 1743-1752.

To demonstrate CBD's ability to target both the (POG)$_2$POA (SEQ ID NO: 45) region and the C-terminal (POG)$_3$ (SEQ ID NO: 44) region, a collagenous peptide [11PROXYL-(POG)$_3$PCG(POG)$_4$]$_3$ (SEQ ID NO: 40) modified to accommodate PROXYL group in the middle (11th position) was synthesized. PROXYL group is covalently joined to the cysteine residue. Due to the presence of the bulky PROXYL group, this peptide is expected to be partially untwisted. The precise degree of under-twisting is not known for the peptide, but mini-collagen with GPX repeats exhibits a moderate under-twisting (κ = -105°). Bella. (2010) *J Struct Biol* 170, 377-391. The bulky PROXYL group will likely induce greater untwisting than κ = -105°. In addition to the eleven amide resonances either line-broaden or shifted, ^{1}H-^{15}N HSQC NMR titrations revealed two distinct phenomena. At lower ratio (0.2:1) amide resonances corresponding to S906, R929, S997, and G998 disappeared from the HSQC spectrum of CBD (Figs. 8E, F and H). Then at higher ratio (0.3:1), additional amide resonances corresponding to V973, G975 and S979 disappeared from the HSQC spectrum of CBD (Figs. 8E, F and H). In

order to cause the disappearance of four residues (S906, R929, S997 and G998), CBD must initially bind to the N-terminal $(POG)_3$ (SEQ ID NO: 44). The disappearance of resonances V973, G975 and S979 can be explained if CBD binds to the C-terminal $(POG)_3$ (SEQ ID NO: 44) of the mini-collagen. However the initial phenomenon signifies that CBD binds preferentially to the under-twisted mid-section to C-terminus.

To demonstrate that PROXYL caused the line broadening and Ala or Cys residues did not, three more control peptides, $[(POG)_4POA(POG)_5]_3$ (SEQ ID NO: 38), $[(POG)_4POA(POG)_5$C-carbamidomethyl]3 (SEQ ID NO: 41), and $[(POG)_3PCG(POG)_4]_3$ (SEQ ID NO: 40) that lack the PROXYL groups were synthesized, and NMR titrations were repeated (Figs. 6F, 8C and 8G, respectively). The titration results were nearly identical with those of $[(POG)io]_3$ (SEQ ID NO: 35). Only the eleven amide resonances were either line broadened or shifted even at 1:1 (mini-collagen:CBD) ratio. These control peptides bound to the same cleft, and PROXYL caused the additional residues to line broaden.

To illustrate if CBD binds only to the partially untwisted site in the middle of the collagen peptide and/or to the C-terminus of mini-collagen, dynamic light scattering experiments (DLS) were performed. DLS experiments provided the stoichiometries of collagen:CBD complexes. The hydrodynamic radius of $[(POG)_4POA(POG)_5$-PROXYL$]_3$(SEQ ID NO: 38):CBD and $[11PR0XYL-(P0G)_3PCG(P0G)_4]_3$(SEQ ID NO: 40):CBD was 3 nm and the apparent molecular weight of the complex was 42±1 kDa, which is similar to those observed for $[(POG),o]_3$(SEQ ID NO: 35):CBD complex (Table 3). Other complexes also exhibited similar values. Thus far, all the mini-collagen and CBD always formed 1:1 complex. CBD binds to either one of the available sites in mini-collagen but does not occupy both sites to form a 1:2 complex.

Table 3: Hydrodynamic radius (RH), apparent molecular weight (Mw), Radius of gyration (Rg) and Maximum particle diameter (Dmax) computed from Dynamic light scattering (DLS) and small angle X-ray scattering (SAXS) for various CBD:collagenous peptides complexes.

No	Complexes	Dynamic Light Scattering (DLS)		Small Angle X-ray Scattering (SAXS)	
		Hydro-dynamic Radius (RH)	Apparent Molecular Weight (Mw)	Radius of Gyration (Rg)	Max Diameter (Dmax)
1	CBD:[(POG)10]3 (SEQ ID NO: 35)	3	43	22.62 ± 0.04	93
2	CBD:[PROXYL-(POG)6POA(POG)3]3 (SEQ ID NO: 36)	3	44	24.67± 0.09	87
3	CBD:[PROXYL-(POG)5POA(POG)4]3 (SEQ ID NO: 37)	3	42	21.08± 0.02	90
4	CBD:[PROXYL-(POG)4POA(POG)5]3 (SEQ ID NO: 38)	3	43	25.48± 0.08	92
	CBD:[(POG)4POA(POG)5]3 (SEQ ID NO: 38)	3	43	24.45± 0.14	85
5	CBD:[PROXYL-(POG)3POA(POG)6]3 (SEQ ID NO: 39)	3	42	21.97± 0.14	94
6	CBD:[(POG)4POA(POG)5C-PROXYL]3 (SEQ ID NO: 41)	3	44	24.09± 0.16	85
	CBD:[(POG)4POA(POG)5]3 (SEQ ID NO: 38)	3	42	24.67± 0.1	84
7	CBD:[11PROXYL-(POG)3PCG(POG)4]3 (SEQ ID NO: 40)	3	42		96
	CBD:[(POG)3PCG(POG)4]3 (SEQ ID NO: 40)	3	43	23.59± 0.05	90

Small angle X-ray scattering experiments (SAXS): The three dimensional molecular shapes of the CBD-collagenous peptide complexes were constructed using SAXS measurements. The main advantage of SAXS measurements is that the experiments are performed in solution under near physiological conditions. In our previous work, these three dimensional molecular envelopes were used to demonstrate asymmetric binding of CBD to the C-terminal $(POG)_3$ (SEQ ID NO: 44) of mini-collagen. The molecular shapes were constructed for complexes of CBD and six different untwisted mini-collagen molecules. In all cases CBD bound to $(POG)_2POA$ (SEQ ID NO: 45) region preferentially to C- terminal $(POG)_3$ (SEQ ID NO: 44) (Figs. 9A-F).

For example the docking model for CBD:$[(POG)_4POA(POG)_5]_3$ (SEQ ID NO: 38Constructed using the crystal structure of CBD (pdb accession code INQD) interacting with $(POG)_2POA$ (SEQ ID NO: 45) region of the untwisted collagen (pdb accession code 1CAG) fit the envelope well (Fig 9B). Although NMR results demonstrated that CBD also binds to the C-terminal $(POG)_3$ (SEQ ID NO: 44) of $[(POG)_4POA(POG)_5$-PROXYL$]_3$ (SEQ ID NO: 38), CBD predominantly binds to the $(POG)_2POA$ (SEQ ID NO: 45) region of the peptide (Figs. 9E and 9F).

Structures derived from SAXS profiles using simulated annealing calculations for [1 1PR0XYL-(P0G) $_3$PCG(P0G) $_4]_3$ (SEQ ID NO: 40) (Figs. 9G and 9H) indicated an additional density that could be attributed to the PROXYL group. The SAXS derived three-dimensional shape of [1 1PR0XYL-(P0G) $_3$PCG(P0G) $_4]_3$(SEQ ID NO: 40):CBD complex superimposes well with either NMR derived complexes *i.e.,* CBD binding to the N-terminal $(POG)_3$ (SEQ ID NO: 44)or to the C-terminal $(POG)_3$ (SEQ ID NO: 44) (Figs. 9G and 9H).

Little structural change of ^{15}N-minicollagen upon CBD binding: The studies thus far suggest that CBD scans the collagen fibril for under-twisted regions. Upon binding to the less structured regions, does it actively unwind collagen? Active unwinding by CBD would facilitate collagenolysis. To investigate two collagenous peptides selectively labeled with ^{15}N near N- or near C-terminus of **[(POG)io]$_3$** (SEQ ID NO: 35) were synthesized (Table 4, peptides A,B), and the structural changes due to the binding of unlabeled CBD were monitored using **^{1}H-^{15}N** HSQC titration.

Table 4: ^{15}N-Labeled Mini-collagen		**SEQ ID NO:**
A	POGPOG*POGPOGPOGPOGPOGPOGPOGPOG	35
B	POGPOGPOGPOGPOGPOGPOGPOGPOG*POG	35
C	POGPOG*POGPOGPOAPOGPOGPOGPOGPOG	38
D	POGPOGPOGPOGPOAPOGPOGPOGPOG*POG	38
* indicates the ^{15}N-labeled Glycine; A indicates Gly→Ala substitution.		

The ^{15}N-Gly labeled peptides exhibited two distinct cross peaks in the ^{1}H-^{15}N HSQC spectrum (Figs. 10A and 10B). Those cross peaks corresponded to unwound monomer and triple helical conformations assigned in earlier NMR studies. Liu, et al.(1996) *Biochemistry* 35, 4306-4313 and Li, et al. (1993) *Biochemistry* 32, 7377-7387. The Gly residue closer to the terminal triplets exhibits both monomer and trimer peaks in the HSQC spectrum, whereas the Gly residue in the middle of the triple helix exhibits a strong trimer cross peak. If CBD is to bend or to cause any unwinding of the triple helix upon binding, we expected the cross peak corresponding to the triple helix to line broaden and disappear on the course of titration, and the cross peak corresponding to the single chain to intensify. However during the course of the titration, CBD did not instigate any changes on the ^{1}H-^{15}N HSQC spectra of the collagenous peptides. Thus CBD bound to C-terminal $(POG)_3$ (SEQ ID NO: 35) imposed little structural changes to the triple helix.

Untwisted mini-collagen molecule selectively labeled with ^{15}N-Gly either at near the N- or C- termini (Table 4C and D) was titrated with unlabeled CBD. Cross peaks corresponding to monomer and triple-helix were identified on the HSQC spectra (Figs IOC and 10D). The titration of unlabeled CBD induced little change in the intensity of either monomer or trimer cross peak. Even upon binding to the partially unwound mini-collagen, CBD does not initiate any further unwinding.

CBD unidirectionally binds to the under-twisted site in the triple helical collagen. CBD may help disband the collagen fibril, but does not unwind the triple helix. Targeting under-twisted regions of tropocollagen may circumvent the energy barrier required for unwinding the triple helices. When CBD is used as a drug delivery molecule, the injected molecule distributes prominently to the end plates of vertebral discs, near the growth plates of tibia and fibula, and also to skin. It could be unloading its payload to the most blood accessible collagen that is undergoing remodeling, thus rich in under-twisted regions.

Example 2: Structural Comparison of ColH and ColG Collagen-Binding Domains

The C-terminal collagen-binding domain (CBD) of collagenase is required for insoluble collagen fibril binding and for subsequent collagenolysis. The high resolution crystal structures of ColG-CBD (s3b) and ColH-CBD (s3) the molecules resemble one another closely (r.m.s.d. C_α = 1.5 A), despite sharing only 30% sequence identity. Five out of six residues chelating Ca^{2+} are conserved. The dual Ca^{2+} binding sites in s3 are completed by a functionally equivalent

aspartate. The three most critical residues for collagen interaction in s3b are conserved in s3. The general shape of the binding pocket is retained by altered loop structures and side-chain positions. Small angle X-ray scattering data revealed that s3 also binds asymmetrically to mini-collagen. Besides the calcium-binding sites and the collagen-binding pocket, architecturally important hydrophobic residues and hydrogen-bonding network around the cw-peptide bond are well-conserved in metallopeptidase subfamily M9B.

Common structural features described above and in Bauer et al. (2012) J Bacteriol November 9 (which is incorporated herein by reference in its entirety), enabled us to update the sequence alignment of the CBD in the M9B subfamily (Fig. 1). Conserved residues are important for one of four reasons: calcium chelation (red), *cis-trans* isomerization of the linker (yellow), collagen-binding (blue) or protein folding (green). Fig. 1 also indicates the strands of the structure along the top of the figure.

The dual calcium-binding site is formed by four chelating residues (Glu899, Glu901, Asn903, and Asp904) within the N-terminal linker, two chelating residues (Asp927 and Asp930) from the β-strand C and invariant Tyrl002 hydrogen- bonds and orients Asp930. Residue numbers used in this paragraph are of s3b. Likewise other supporting cast such as Gly921 is conserved in the middle of β-strand strategically placed to make room for Glu899. The dual calcium chelation site is fashioned sometimes by functionally equivalent residues. As mentioned, Asp897 of s3 acts equivalently to Asp927 of s3b. Asp897 equivalents are tentatively identified in *B. brevis* s3a and s3b, *C. botulinum* A3 s3a and *C. histolyticum* ColG s3a. Tridentate and divalent Asp and Glu residues are conserved with only *C. sordellii* s3a as the exception. The monodentate Asp904 residue is sometimes substituted by Asn. For those substituted, the net charge of the dual calcium site is neutral rather than -1.

The peptide between residues 901-902 has *cis* conformation in the *holo* state for both s3b and s3. The position 902 in other CBD molecules is Pro, Asp or Asn. Pro frequently succeeds the peptide bond to ease *trans-cis* isomerization. The s3 molecule has Pro. In s3b, OD of Asn902 hydrogen-bonds with the main-chain N of Asp904. The hydrogen-bond is critical for the peptide isomerization. Spiriti and van der Vaart. (2010) Biochemistry 49:5314-5320, which is incorporated herein by reference in its entirety. For the remainder of CBD molecules with Asp at the position, OD of Asp could play the same role as that of Asn902. Other hydrogen-bonds identified by simulation studies important in stabilizing the transition states are well conserved.

These donor-acceptor pairs in s3 and s3b are tabulated (Table 5). Calcium ions could catalyze the isomerization in all the CBD molecules and their transition states and catalytic mechanism may look very similar.

Table 5: Hydrogen-bonds important in *trans-cis* peptide isomerization in s3b and their counterparts in s3.

Important H-bonds in s3b for transition state formation	Corresponding H-bonds in s3
T910_OG1...N903_NH2	S879_OG1...N872_ND2
T910_OG1...N900_N	S879_OG1...K86_N
E899_OE1...N903_ND2	E868_OE1...N872_ND2
E899_OE2...S922_N	E868_OE2...T891_N
N902_OD1...D904_N	NA (N902 replaced with P871)
D930_OD2...Y1002_OH	D939_OD2...Y97_OH
Y1002_OH...Y932_OH	NA (Y932 replaced with F901)

Non-functional residues that are important in either folding or architectural stability are conserved. Hydrophobic residues packed between the β-sheets are better conserved if they are located in the vicinity of functionally critical residues. For example, invariant Trp956 of strand E is packed between the β-sheets. The residues flanking (Thr955 & Thr957) interact with mini-collagen. Tyr932 is packed between the sheets and helps positioning Tyrl 002. Residues at tight turns are conserved as well. Gly975 is well conserved to allow a type IF turn in s3b. Gly942 (Gly975 equivalent) in s3 allows Asp941 side-chain to stabilize the reverse turn. A highly conserved six-residue stretch, between residues 986 and 991, adopts a tight turn and precedes the functionally important strand H. The region is well ordered in the crystal structures with low B-factors, and is the least dynamic based on NMR and limited proteolysis MALDI-TOF MS (25). Philominathan, et al. (2009) J Biol Chem 284:10868-10876 and Sides et al. J Am Soc Mass Spectrom. (2012) 23(3):505-19 both of which are incorporated herein by reference in their entireties. The main-chain carbonyl and amino groups of Arg985 hydrogen-bond with OH of Tyr989 to stabilize the turn. Only Gly987 can make room for the bulky Tyr989 side chain. Tyr990 packs against the invariant Ala909 and conserved 3_{10} helix.Ala909 is at the base of the linker that undergoes α-helix->P-strand transformation. The tight turn may ensure that collagen interacting Leu992, Tyr994, and Tyr996 would be correctly positioned. Tyr994 is the most critical residue in interacting with collagenous peptides. Wilson, et al. (2003) EMBO J 22:1743-1752. The strands adjacent to strand H, *i.e.* strands C and E, are very well conserved. The three antiparallel strands mold the collagen-binding pocket. Strand F staples the β-sheets by interacting with both sheets. The β-strand first interacts in an antiparallel orientation with strand

E then breaks its direction at Gly971 to interact with strand G. In place of Gly971, Ala or Pro is found at the location where the strand switches its allegiance. The dual interaction of the strand helps positioning Tyr970 to interact with mini-collagen.

Three residues shown to interact strongly with mini-collagen are conserved. The invariant Tyr994 and well conserved Tyr970 andTyr996 constitute the "hot spot". Y994A mutation lost binding capability. Since Y994F resulted in 12-fold reduction in binding to mini-collagen, the hydroxyl group of Tyr994 may interact with collagen through a hydrogen-bond. Tyr996, which is a critical residue in binding mini-collagen, is not so well conserved. Y996A caused 40-fold reduction in binding to the mini-collagen. Y996 is s3b is replaced with Phe in s3, though both side chains have identical orientation. In other CBD molecules, an aromatic residue, such as Phe or His, is sometimes found at the site. Y970A results in 12-fold reduction in binding to mini-collagen. Thr957 was found to interact with mini-collagen by ^{15}N-HSQC-NMR titration. The β-branched amino acid residues or Leu are found at the positions equivalent to Thr957 in most of the CBDs. Six other residues were identified by ^{15}N-HSQC-NMR titration to interact with mini-collagen are not very well conserved. Since divergent CBDs (s3 and s3b) adopted a similar saddle-shaped binding pocket, other CBDs may also adopt similar collagen-binding strategy.

Divergent CBD could target different collagen sequences and could possibly target different collagen types; however, this structural study suggest otherwise. Rather, all the CBD domains may bind similarly to an under-twisted region such as the C-terminus of a collagen fibril. The C-terminus of type I collagen is exposed in the fibril surface based on X-ray fiber diffraction experiments, and it is the most accessible site for the bacterial coUagenase to initiate assaults. However CBD binding only at the C-terminal region of tropocollagen is unfounded. Gold particle-labeled tandem ColG-CBD (s3a-s3b) labeled with gold particle bound to type I collagen fibrils exhibited no periodicity. In the collagen fibrils, the molecules are staggered from each other by about 67nm. Therefore CBD could target partially under-twisted regions in the middle of a tropocollagen that are also vulnerable for assaults.

Much like s3b, s3 is both compact, and extremely stable in the presence of physiological Ca^{2+}. Thus, the enzyme could degrade extracellular matrix for prolonged time. The linker that induced structural transformation is a common feature found in M9B coUagenase. It could act as

Ca^{2+} sensor to trigger domain rearrangement as means of enzyme activation. Ca^{2+} concentration in extracellular matrix is higher than that inside a bacterium. Both s3 and s3b bind similarly to a mini-collagen, thus M9B collagenase molecules could initiate collagenolysis from analogous structural features in various collagen fibril. Fusion protein of any CBD derived from M9B collagenase and a growth factor should result in comparable clinical outcome.

Example 3: CBD-PTH agonist spurs hair growth and CBD-PTH antagonist inhibits hair growth

In-Vitro Characterization of CBD-Linked PTH Compounds: Collagen binding of each peptide was verified in flow-through collagen binding assays as previously described in U.S. Patent Publication No. 2010/0129341, which is incorporated herein by reference in its entirety. PTH-CBD, consisting of the first 33 amino acids of PTH linked directly to the collagen binding domain (SEQ ID NO: 1), was the most potent agonist, having a similar effect to that of PTH(l-34) (SEQ ID NO: 7) on cAMP accumulation. Ponnapakkam et al. (2011) Calcif 88:511-520. Epub 2011 Apr 2022. Among the antagonists, PTH(7-33)-CBD (SEQ ID NO: 10) had the best combination of low intrinsic activity and high receptor blockade (not shown), similar to those seen in other PTH antagonists, including those used in hair growth studies. Peters, et al. (2001) J Invest Dermatol 117:173-178.

In-Vivo Distribution of PTH-CBD: Tissue distribution was assessed by administering ^{35}S-labelled PTH-CBD via subcutaneous injection, followed by whole mount frozen and whole-body autoradiography. PTH-CBD with a phosphorylation site between PTH(l-33) and the CBD was purified, activated and labeled with [gamma-35] ATP as described previously. Tamai et al. (2003) Infect Immun. 71:5371-5375. Approximately 10.8 meg of ^{35}S-PTH-CBD (122 kem/meg) was injected subcutaneously in 7 week-old mice (32-35g). Mice were sacrificed at 1 hour or 12 hours post-injection, and then frozen in dry ice-acetone. Frozen sections (50 μm) were prepared with an autocryotome, dried at -20°C, and exposed to an image plate for 4 weeks. There appeared to be an initial distribution of ^{35}S-PTH-CBD to a broad area of skin around the site of injection, followed by a rapid redistribution to the skin of the entire animal, as well as to several other tissues (i.e. bone, intestine, bladder) (Fig. 11). PTH-CBD thus showed the desired properties of distribution and retention to skin with subcutaneous administration.

PTH-CBD Reverses Hair Loss in Chemotherapy-induced Alopecia in Mice:

We compared efficacy of CBD linked PTH agonists and antagonists in chemotherapy-induced alopecia, utilizing an experimental design published by Peters, et al., for non-CBD linked PTH compounds. Peters, et al. (2001) J Invest Dermatol 117:173-178. C57BL/6J mice (Jackson Laboratories, Bar Harbor, Maine) were depilated to synchronize the hair follicles, and cyclophosphamide (CYP, 150 mg/kg) was administered on day 9 to maximize the chemotherapy-induced damage. The agonist (PTH-CBD) and the antagonist (PTH(7-33)-CBD) were administered 2 days prior to chemotherapy, and given the long-term retention of the compounds in the skin, we administered only a single dose to cover the timing of the multiple injections of PTH agonist and antagonist in the study by Peters, et. al. The administered dose of CBD-linked compounds (320 mcg/kg) is well tolerated in mice. Ponnapakkam et al. (201 1) Calcif 88:51 1-520. Epub 201 1 Apr 2022.

The results of the photodocumentation record indicate that the agonist, PTH-CBD, was far more effective at stimulating hair growth than was the antagonist (Fig. 12). Histological examination revealed morphological changes in the hair follicles after CYP therapy, which were more superficially located and exhibited clumped melanocytes around the bulb, characteristics of the dystrophic anagen and catagen phase (Fig. 13). While the antagonist PTH(7-33)-CBD had no beneficial effect, treatment with the agonist PTH-CBD led to deeper rooting and reduced melanocyte clumping, thus reversing the dystrophic changes. Counts of anagen VI hair follicles per high-powered field (HPF) were compared between groups; animals treated with PTH-CBD had a higher number of hair follicles, approaching those of animals which did not receive chemotherapy (Fig. 14), while the antagonist PTH(7-33)-CBD had no beneficial effect.

Importantly, we saw no evidence of adverse effects from PTH-CBD administration. While PTH injections are known to elevate blood calcium and can cause kidney stones, PTH-CBD had no effect on serum calcium. In addition, there was no evidence of excess hair length on the body or of excess hair growth on the ears and tail, where a full coat is normally not present. The effects of PTH-CBD on hair growth have been confirmed in models of chemotherapy-induced alopecia without depilation, which more closely mimic clinical protocols.

Quantification of Effects of PTH-CBD in Chemotherapy-induced Alopecia: We followed these studies by comparing the effects of different doses of PTH-CBD in chemotherapy- induced alopecia. In these studies, we applied the injections more distally on the back and applied a gray-scale analysis to quantify the amount of hair growth. Injecting more

distally in the back allows us to compare regrowth of hair after PTH-CBD treatment with less interference from the normal hair regrowth, which normally proceeds from head to tail in mice. The results are shown in Fig. 15, indicating a dose-dependent effect on hair regrowth both qualitatively and quantitatively.

Chemotherapy-induced Alopecia without Depilation: While the depilated model of chemotherapy-induced alopecia provides a uniform model for comparison of drug effects, the depilation process is known to cause hair follicle injury, and may alter the response of the animals to the PTH-CBD administration. We therefore tested the effects of PTH-CBD in another model of chemotherapy-induced alopecia, where the animals were given 3 courses of cyclophosphamide therapy (50 mg/kg/wk), similar to the usual manner in which cancer patients might be treated. In this model, it takes much longer (4-6 months) for alopecia to develop. Animals that received a single dose of PTH-CBD (320 mcg/kg subcutaneous) prior to the first cycle did not develop hair loss as shown in Figure 16.

In a second study, we compared the effects of PTH-CBD when given prophylactically, at the time of the first cycle of chemotherapy, vs. therapeutically, after the hair loss had developed. While PTH-CBD was effective in both instances, the effects were more prominent when given prophylactically. This is evident both visually and quantitatively in Fig. 17, using the same grey scale analysis used in our dose-response study.

Depilation Alopecia: The agonist PTH-CBD appears to increase hair growth by increasing the number of anagen phase hair follicles. As such, there is no reason to believe that hair growth effects should be limited to the chemotherapy model. We therefore tested both PTH-CBD and antagonist compound, PTH(7-33)-CBD, after removing hair from C57/BL6J mice by waxing (Fig. 18). The results were quite interesting; agonist (PTH-CBD) treated animals had earlier anagen eruption (day 7 vs. day 9 for vehicle controls), and exhibited more complete regrowth of hair by the end of the study (day 18). Antagonist (PTH(7-33)-CBD) treated animals also had an early anagen eruption, but the hair growth which followed was markedly curtailed, and the hair cycle was arrested after this point, resulting no further observed regrowth of hair. Thus, it appears that agonist therapy is acting to promote more rapid regrowth of hair by promoting more rapid transition to the anagen phase, while the antagonist inhibited hair regrowth by blocking this transition.

PTH-CBD is a fusion protein of the first 33 amino acids of parathyroid hormone (PTH) and a bacterial collagen binding domain. The collagen binding activity causes PTH-CBD to be retained at its site of action in the dermal collagen, maximizing efficacy and reducing systemic side-effects. PTH-CBD stimulates hair growth by causing hair follicles to enter an anagen VI or growth phase, presumably by activating WNT signaling and increasing production of beta-catenin. We therefore plan to conduct the following additional studies to confirm this mechanism of action and to determine the effect of PTH-CBD in two distinct genetic mouse models with WNT signaling inhibition. These data will be used in formulating clinical trials for PTH-CBD as a therapy for alopecia.

Alopecia Areata: Alopecia Areata is a disease of patchy hair loss due to autoimmune destruction of the hair follicles. We tested the efficacy of PTH-CBD in promoting regrowth of hair in an animal model of alopecia areata, the engrafted C3H/Hej mouse. In this model, hair loss develops variably over the first 2 months of life. Shown in Fig. 19 is the results of a single dose of PTH-CBD (320 mcg/kg subcutaneous) administered into the engrafted site, the center of the back, where there was maximal hair loss. Compared to vehicle control animals, which continued to lose hair at this site, animals receiving PTH-CBD began to show regrowth of hair within the next 1-4 days. Importantly, the response was found to be sustained during the 2 month course of the experiment.

Example 4: **CBD-PTH can prevent or treat hyperparathyroidism**

In this experiment, rats had their ovaries surgically removed at age 3 months. At age 9 months, rats were injected with either a single dose of PTH-CBD (320 mcg/kg) or vehicle control. Animals were sacrificed 6 months after therapy (age 15 months). Human intact PTH levels were measured to assess serum levels of PTH-CBD, and were found to be undetectable in both groups. Serum calcium was measured and there were no differences between groups (Vehicle: 13.5 +/- 1.1 vs. PTH-CBD: 14.3 +/- 1.1 mg/dl, NS). Rat intact PTH levels were measured to assess endogenous PTH production, and PTH-CBD suppressed the normal increase in endogenous PTH levels seen in aged, ovarectomized rats. These findings indicate that a single injection of PTH-CBD can provide long-term suppression of endogenous PTH production, preventing the normal rise seen with age in the ovarectomized rat model, and thus may serve as a therapy for hyperparathyroidism.

CLAIMS

We claim:

1. A method of delivering a therapeutic agent comprising: administering a composition comprising a bacterial collagen-binding polypeptide segment linked to a therapeutic agent to a subject in need of treatment with the therapeutic agent, wherein the therapeutic agent is not a PTH/PTHrP receptor agonist or antagonist, and wherein the bacterial collagen-binding polypeptide segment delivers the agent to sites of partially untwisted or under-twisted collagen.

2. The method of claim 1, wherein the therapeutic agent is being delivered to treat a collagenopathy.

3. A method of treating a collagenopathy comprising administering a composition comprising a bacterial collagen-binding polypeptide segment linked to a PTH/PTHrP receptor agonist to a subject, wherein the bacterial collagen-binding polypeptide segment delivers the agent to sites of partially untwisted or under-twisted collagen.

4. The method of claim 3, wherein the PTH/PTHrP receptor agonist comprises residues 1-33 of SEQ ID NO: 1, PTH (SEQ ID NO: 7), residues 1-14 of SEQ ID NO: 1, residues 1-34 of SEQ ID NO: 7 or a fragment of at least 8 consecutive amino acids from residues 1-34 of SEQ ID NO: 7.

5. The method of any of claims 3-4, wherein the PTH/PTHrP receptor agonist is a polypeptide and the N-terminus of the collagen-binding polypeptide segment is linked directly or through a linker polypeptide segment to the C-terminus of the PTH/PTHrP receptor agonist polypeptide.

6. The method of any one of claims 3-5, wherein the composition has at least 50% greater activity in the subject than PTH(l-34) administered alone.

7. The method of any one of claims 2-6, wherein the collagenopathy is selected from the group consisting of osteogenesis imperfecta, Stickler's syndrome, Ehlers-Danlos syndrome, Alport's syndrome, Caffey's disease, and localized collagen or cartilage damage.

8. The method of any one of claims 1-7, wherein the therapeutic agent is an agent capable of promoting bone growth, decreasing inflammation, or promoting collagen stability.

9. The method of any one of claims 1-8, wherein the therapeutic agent is selected from the group consisting of BMP-2, BMP-3, FGF-2, FGF-4, anti-sclerostin antibody, growth hormone, IGF-1, VEGF, TGF-b, KGF, FGF-10, TGF-a, TGF-bl, TGF-b receptor, GM-CSF, EGF, PDGF and connective tissue growth factors.

10. The method of any one of claims 1-9, wherein the bacterial collagen-binding polypeptide segment comprises a collagen-binding polypeptide derived from an M9 peptidase selected from the group consisting of *Clostridium*, *Bacillus* and *Vibrio*, one of SEQ ID NOs: 13-34 or a fragment thereof, residues 34-158 of SEQ ID NO: 1, a fragment of at least 8 consecutive amino acids from residues 34-158 of SEQ ID NO: 1, or a peptide that is at least 90% identical to residues 34-158 of SEQ ID NO: 1 or SEQ ID NOs: 13-34.

11. The method of any one of claims 1-10, wherein the collagen-binding polypeptide segment and the therapeutic agent are chemically cross-linked to each other or are polypeptide portions of a fusion protein.

12. The method of any one of claims 1-11, wherein the therapeutic agent is a polypeptide and the N-terminus of the collagen-binding polypeptide segment is linked directly or through a linker polypeptide segment to the C-terminus of the therapeutic agent polypeptide.

13. The method of any one of claims 1-12, wherein the composition has at least 50%> greater activity in the subject than the therapeutic agent administered alone.

14. The method of any one of claims 1-13, wherein the composition is administered intramuscularly, intradermally, intravenously, subcutaneously, intraperitoneally, topically, orally, parenteral, or intranasally.

15. The method of any one of claims 1-14, wherein the subject is a human.

16. The method of any one of claims 1-15, wherein the composition is administered in aqueous solution at pH below about 5.0.

17. The method of any one of claims 1-16, wherein the composition is administered in aqueous solution at pH above about 6.0.

18. A method of treating alopecia that is not chemotherapy-induced or increasing hair growth in a subject in need of hair growth comprising administering a composition comprising a bacterial collagen-binding polypeptide segment linked to a PTH/PTHrP receptor agonist to a subject to increase hair growth.

19. The method of claim 18, wherein the alopecia is alopecia areata.

20. The method of claim 18, wherein the alopecia is related to male pattern baldness or polycystic ovarian syndrome.

21. The method of any one of claims 18-20, wherein the composition is administered locally.

22. The method of claim 21, wherein the composition is administered topically

23. A method of treating hyperparathyroidism comprising administering a composition comprising a bacterial collagen-binding polypeptide segment linked to a PTH/PTHrP receptor agonist to a subject in need of treatment for hyperparathyroidism.

24. The method of claim 23, wherein the composition is administered intramuscularly, intradermally, intravenously, subcutaneously, intraperitoneally, topically, orally, parenteral, or intranasally.

25. The method of any one of claims 18-24, wherein the bacterial collagen-binding polypeptide segment comprises a collagen-binding polypeptide derived from an M9 peptidase selected from the group consisting of *Clostridium, Bacillus* and *Vibrio,* one of SEQ ID NOs: 13-34 or a fragment thereof, residues 34-158 of SEQ ID NO: 1, a fragment of at least 8 consecutive amino acids from residues 34-158 of SEQ ID NO: 1, or a peptide that is at least 90% identical to residues 34-158 of SEQ ID NO: 1 or SEQ ID NOs: 13-34.

26. The method of any one of claims 18-25, wherein the PTH/PTHrP receptor agonist comprises residues 1-33 of SEQ ID NO: 1, PTH (SEQ ID NO: 7), residues 1-14 of SEQ ID NO: 1, residues 1-34 of SEQ ID NO: 7 or a fragment of at least 8 consecutive amino acids from residues 1-34 of SEQ ID NO: 7.

27. The method of any of claims 18-26, wherein the PTH/PTHrP receptor agonist is a polypeptide and the N-terminus of the collagen-binding polypeptide segment is linked directly or through a linker polypeptide segment to the C-terminus of the PTH/PTHrP receptor agonist polypeptide.

28. The method of any one of claims 18-26, wherein the collagen-binding polypeptide segment and the therapeutic agent are chemically cross-linked to each other or are polypeptide portions of a fusion protein.

29. The method of any one of claims 18-28, wherein the composition has at least 50% greater activity in the subject than PTH(l-34) administered alone.

30. The method of any one of claims 18-29, wherein the subject is a human.

31. The method of any one of claims 18-30, wherein the composition is administered in aqueous solution at pH below about 5.0.

32. The method of any one of claims 18-30, wherein the composition is administered in aqueous solution at pH above about 6.0.

33. A method of slowing hair growth comprising administering a composition comprising a bacterial collagen-binding polypeptide segment linked to a PTH/PTHrP receptor antagonist to a subject to slow hair growth.

34. The method of claim 33, wherein the composition is administered locally.

35. The method of claim 34, wherein the composition is administered topically.

36. The method of any one of claims 33-35, wherein the bacterial collagen-binding polypeptide segment comprises a collagen-binding polypeptide derived from an M9 peptidase selected from the group consisting of *Clostridium, Bacillus* and *Vibrio,* one of SEQ ID NOs 13-34 or a fragment thereof, residues 34-158 of SEQ ID NO: 1, a fragment of at least 8 consecutive amino acids from residues 34-158 of SEQ ID NO: 1, or a peptide that is at least 90% identical to residues 34-158 of SEQ ID NO: 1 or SEQ ID NOs: 13-34.

37. The method of any one of claims 33-36, wherein the PTH/PTHrP receptor antagonist comprises residues 7-33 of SEQ ID NO: 7, residues 7-14 of SEQ ID NO: 7, a fragment of at least 8 consecutive amino acids from residues 7-34 of SEQ ID NO: 7 or residues ((-1)-33) ofPTH.

38. The method of any of claims 33-37, wherein the PTH/PTHrP receptor antagonist is a polypeptide and the N-terminus of the collagen-binding polypeptide segment is linked directly or through a linker polypeptide segment to the C-terminus of the PTH/PTHrP receptor antagonist polypeptide.

39. The method of any one of claims 33-37, wherein the collagen-binding polypeptide segment and the therapeutic agent are chemically cross-linked to each other or are polypeptide portions of a fusion protein.

40. The method of any one of claims 33-39, wherein the composition has at least 50% greater activity in the subject than PTH(7-33) administered alone.

41. The method of any one of claims 33-40, wherein the subject is human.

Figure 1

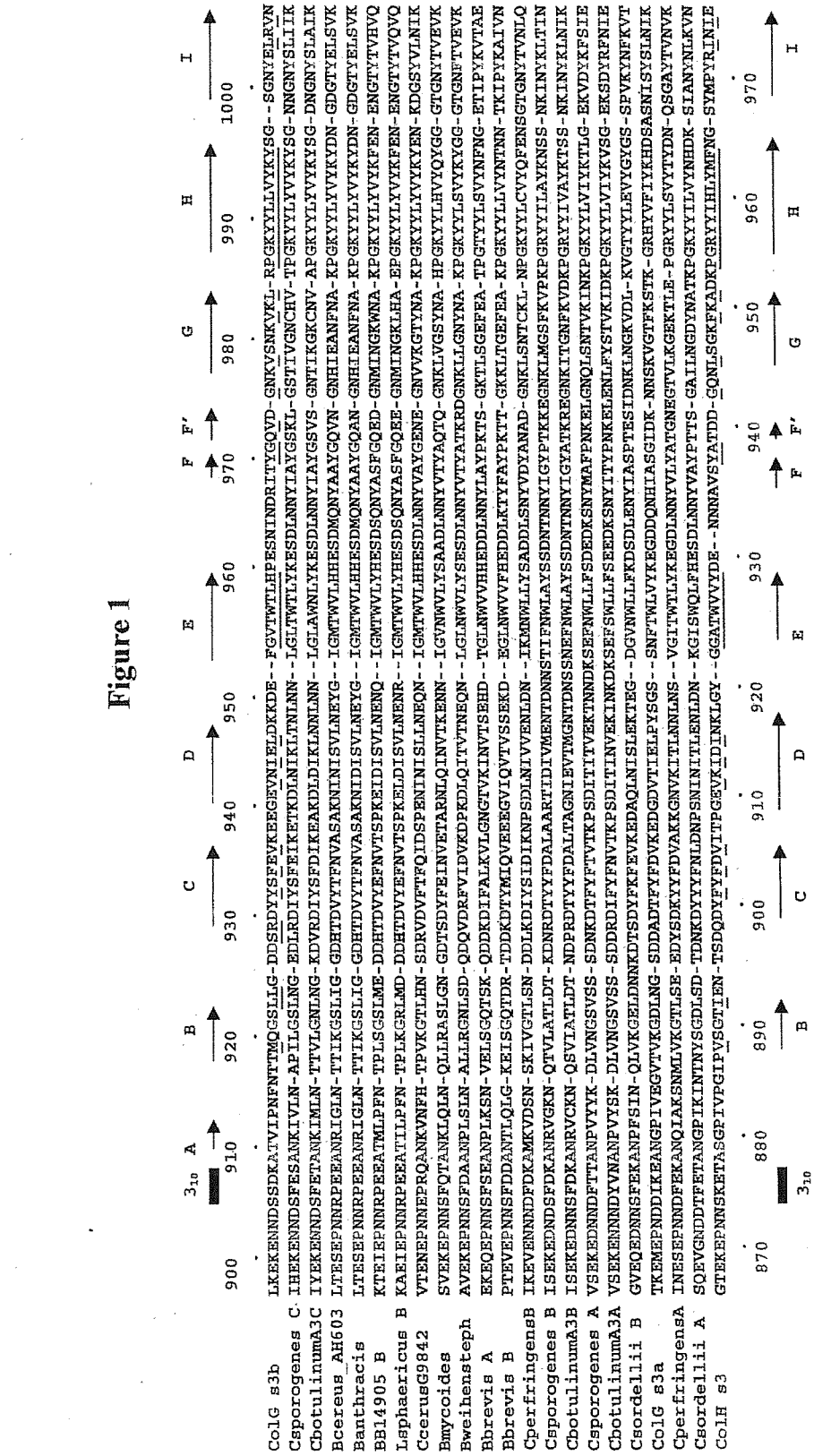
3₁₀ A
B
C
D
E
F F'
G
H
I
900
910
920
930
940
950
960
970
980
990
1000
ColG s3b LKEKENNDSSDKATVIPNFNTTMQGSLLG-DDSRDYTSFEVKEEGEVNIELDKKDE--FGVTWTLHPESNINDRITYGQVD-GNKVSMKVKL--RPGKYYLLVYKKYSG--SGNYELRVN
Csporogenes C IHEKENNDSFESANKIVLN-APILGSLNG-EDLRDIYSFEIKETKDLNIKLTNLNNN--LGLTWTLYKESDLNNYIAYGSKL-GSTIVGNCHV-TPGKYYLYVVKYYSG-NNGNYSLIIK
CbotulinumA3C IYEKENNDSFETANKIMLN-TTVLGNLNG-KDVRDIYSFDIKEAKDLDIKLNNLNNN--LGLAWNLYKESDLNNYIAYGSVS-GNTIKGKCNV-APGKYYLYVVKYSG-DNGNYSLAIK
Bcereus AH603 LTESEPNNNRPEEANRIGLN-TTIKGSLIG-GDHTDVYTFNVASAKNINISVLNEYG--IGMTWVLHHESDMQNYAAYGQVN-GNHIEANFNA-KPGKYYLYVVKYDN-GDGTYELSVK
Banthracis LTESEPNNNRPEEANRIGLN-TTIKGSLIG-GDHTDVYTFNVASAKNIDISVLNEYG--IGMTWVLHHESDMQNYAAYGQAN-GNHIEANFNA-KPGKYYLYVVKYDN-GDGTYELSVK
BB14905 B KTEIEPNNNRPEEATMLPFN-TPLSGSLME-DDHTDVYEFNVTSPKEIDISVLNENQ--IGMTWVLYHESDSQNYASFGQED-GNMINGKWNA-KPGKYYLIYVKKFEN-ENGTYTVHVQ
Lsphaericus B KAEIEPNNNRPEEATILPFN-TPLKGRLMD-DDHTDVYEFNVTSPKELDISVLNENR--IGMTWVLYHESDSQNYASFGQEE-GNMINGKLHA-EPGKYYLYVVKKFEN-ENGTYTVQVQ
Ccerus69842 VTENEPNNNERPQANKVNFH-TPVKGTLHN-SDRVDVFTFQIDSPENINISLLNEQN--IGMTWVLHHESDLNNYVAYGENE-GNVVKGTYNA-KPGKYYLYVYKYEN-KDGSYVLNIK
Bmycoides SVEKEPNNNSFQTANKLQLN-QLLRASLGN-GDTSDYFEINVETARNLQINVTKENN--IGVNWVLYSAADLNNYVTYAQTQ-GNKLVGSYNA-HPGKYYLHVVQYGG-GTGNYTVEVK
Bweihensteph AVEKEPNNSFDAANPLSLN-ALLRGNLSD-QDQVDRFVIDVKDPKDLQITVTNEQN--LGLNWVLYSESDLNNYVTYATKRDGNKLLGNYNA-KPGKYYLSVVKYGG-GTGNFTVEVK
Bbrevis A EKEQEPNNSPSEANPLKSN-VELSGQTSK-QDDKDIFALKVLGNGTVKINVTSEHD--TGLNWVVHHEDDLNNYLAYPKTS-GKTLSGEFEA-TPGTYYLSVVNFNG-ETLPYKVTAE
Bbrevis B PTEVEPNNSFDDANTLQLG-KEISGQTDR-TDDKDTYMIQVEEEGVIQVTVSSEKD--EGLNWVVFHEDDLKTYFAYPKTT-GKKLTGEFEA-KPGKYYLLVYNTNN-TKIPYKATVN
CperfringensB IKEVENNNDFDKAMKVDSN-SKIVGTLSN-DDLKDIYSIDIKNPSDLNIVVENLDN--IKMNWLLYSADDLSNYVDYANAD-GNKLSNTCKL-NPGKYYLCVYQFENSGTGNYTVNLQ
Csporogenes B ISEKEDNDSFDKANRVGKN-QTVLATLDT-KDNRDTYYFDALAARTIDIVMENTDNNSTIFNWLAYSSDNTNNYIGYPTKKEGNKLMGSFKVPKPGRYYILAYKNSS-NKINYKLTIN
CbotulinumA3B ISEKEDNNSFDKANRVCKN-QSVIATLDT-NDPRDTYYFDALTAGNIEVTMGNTDNSSNEFNWLAYSSDNTNNYIGYATKREGNKTIGNFKVDKPGRYYIVAYKTSS-NKINYKLNIK
Csporogenes A VSEKEDNNDFTTANPVYYK-DLVNGSVSS-SDNKDTFYFTVEKTNNDKSEFNWLLFSDEDKSNYMAFPNKELGNQLSNTVKINKPGKYYLVIYKTLG-EKVDYKFSIE
CbotulinumA3A VSEKENNNDYVNANPVYSK-DLVNGSVSS-SDDRDIFYFNVTKPSDITINVEKINKDKSEFSWLLFSEEDKSNYITYPNKELENLFYSTVKIDKPGKYYLVIYKVSG-EKSDYRFNIE
Csordellii B GVEQEDNNSFEKANPFSIN-QLVKGELDNNKDTSDYFKFEVKEDAQLNISLEKTEG--DGVNWLLFKDSDLENYIASPTESIDNKLNGKVDL-KVGTYYLEVYGYGS-SPVKYNFKVT
ColG s3a TKEMEPNDDIKEANGPIVEGVTVKGDLNG-SDDADTFYFDVKEDGDVTIELFYSGS--SNFTWLVYKEGDDQNHIASGIDK-NNSKVGTFKSTK-GRHIVFIYKHDSASNISYSLNIK
CperfringensA INESEPNNDFEKANQIAKSNMLVKGTLSE-EDYSDKYYFDVAKKGNVKITLNNNLNS--VGITWTLYKEGDLNNYVLIATGNEGTVLKGEKTLE-PGRYYLSVYTYDN-QSGAYTVNVK
Csordellii A SQEVGNDDTFETANGPIKINTNYSGDLSD-TDNKDYTYFNLDNPSNINITLENLDN--KGISWQLFHESDLNNYVAYPTTS-GAILNGDYNATKPGKYYILVYNHDK-SIANYNLKVN
ColH s3 GTEKEPNNSKETASGPIVPGIPVSGTIEN-TSDQDYFYFDVTTPGEVKIDINKLGY--GGATVVYDE--NNNAVSYATDD-GQNLSGKFKADKPGRYYIHLYMFNG-SYMPYRINIE
870
880
890
900
910
920
930
940
950
960
970
3₁₀
B
C
D
E
F F'
G
H
I

Figure 2

PROXYL-$(POG)_6POA(POG)_3$

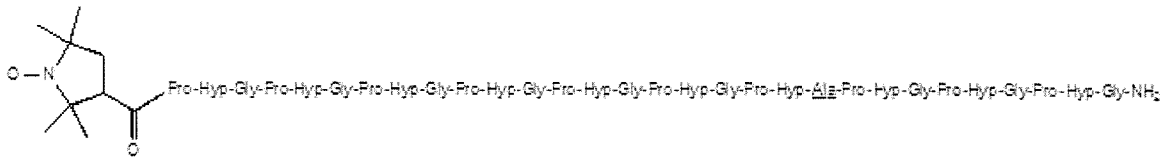

PROXYL-$(POG)_5POA(POG)_4$

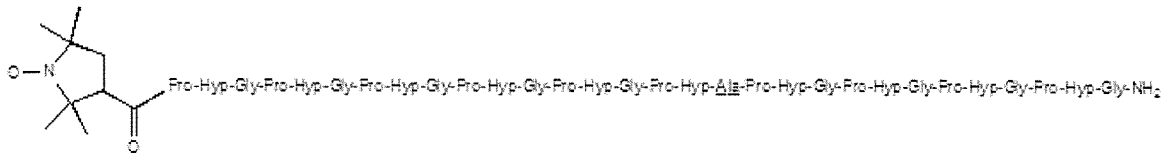

PROXYL-$(POG)_4POA(POG)_5$

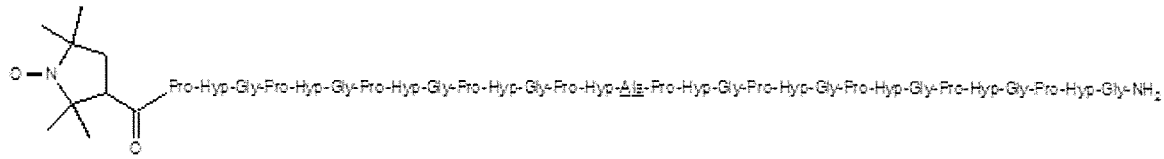

PROXYL-$(POG)_3POA(POG)_6$

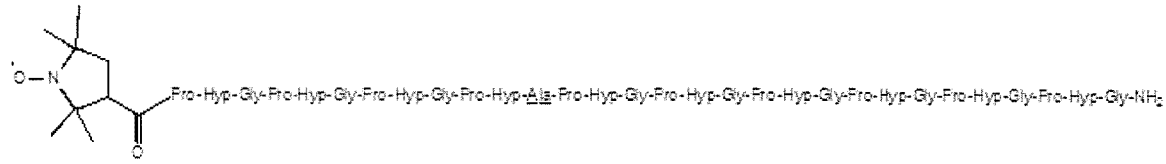

$(POG)_4POA(POG)_5C$-PROXYL

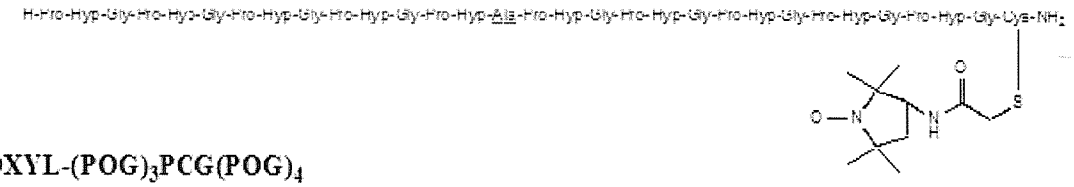

[11]PROXYL-$(POG)_3PCG(POG)_4$

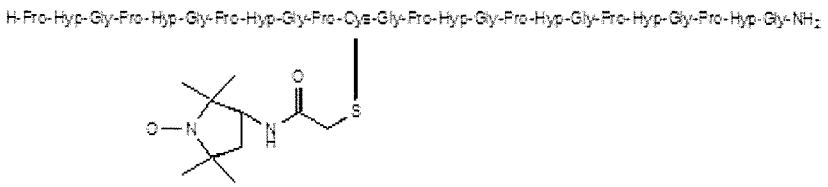

Figure 3A

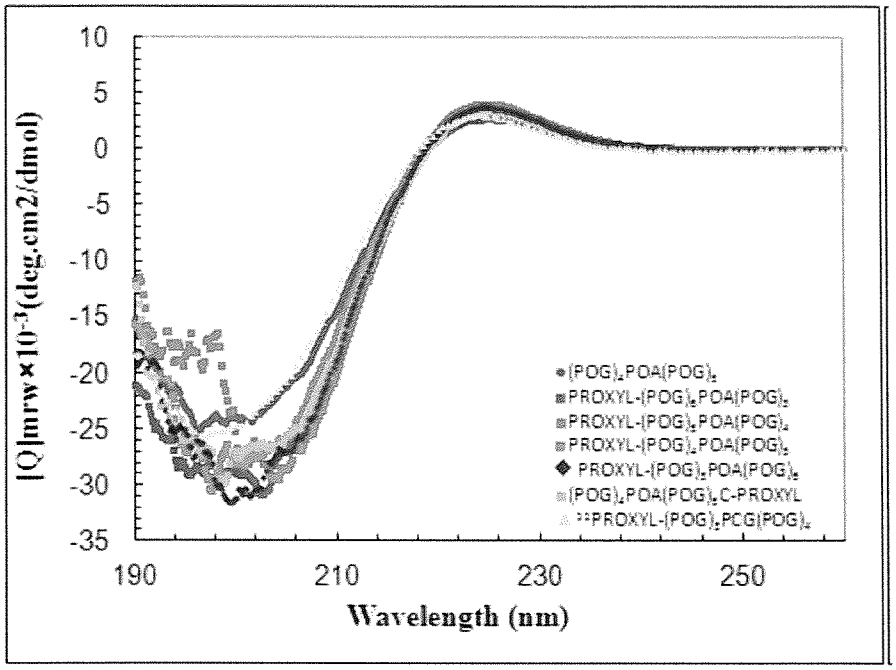

Figure 3B

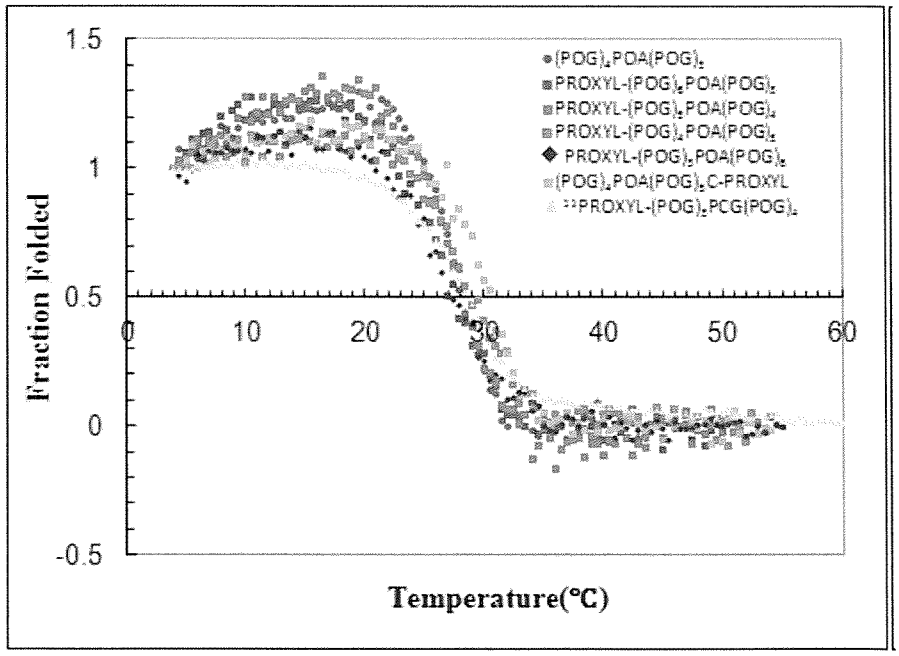

Figure 4

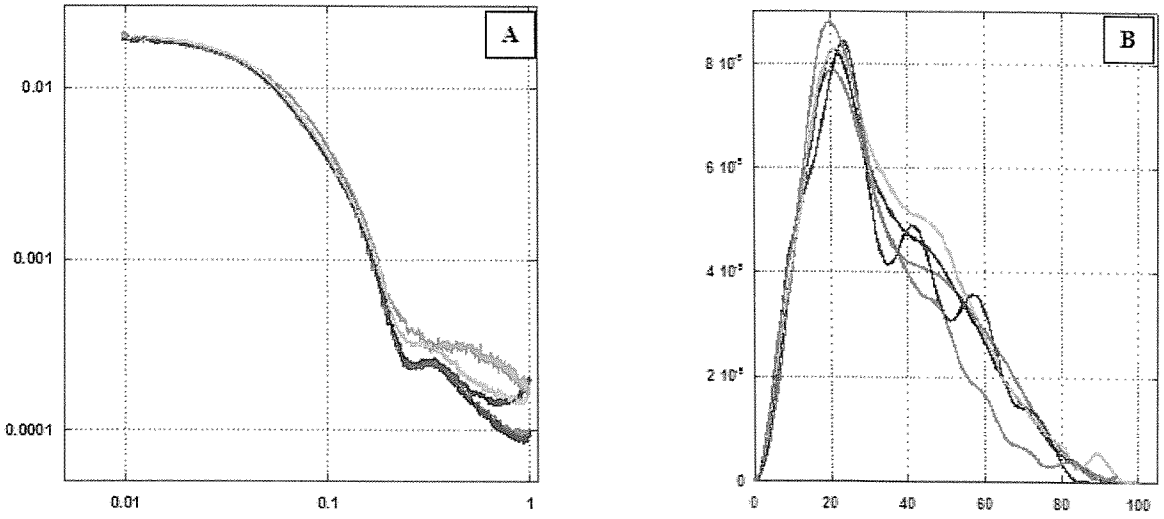

Figure 5

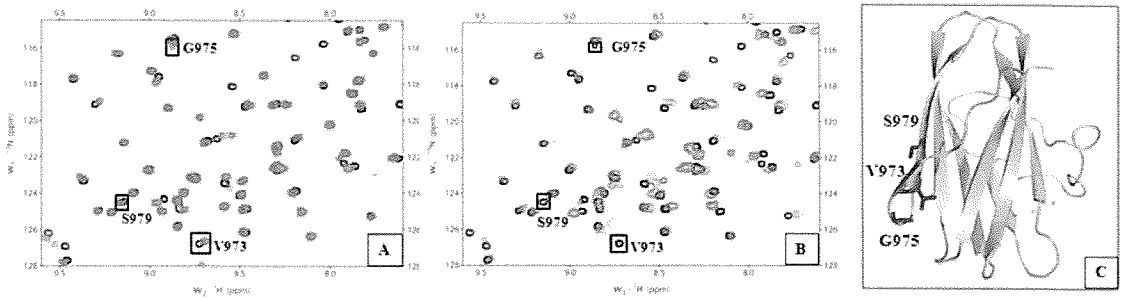

Figure 6

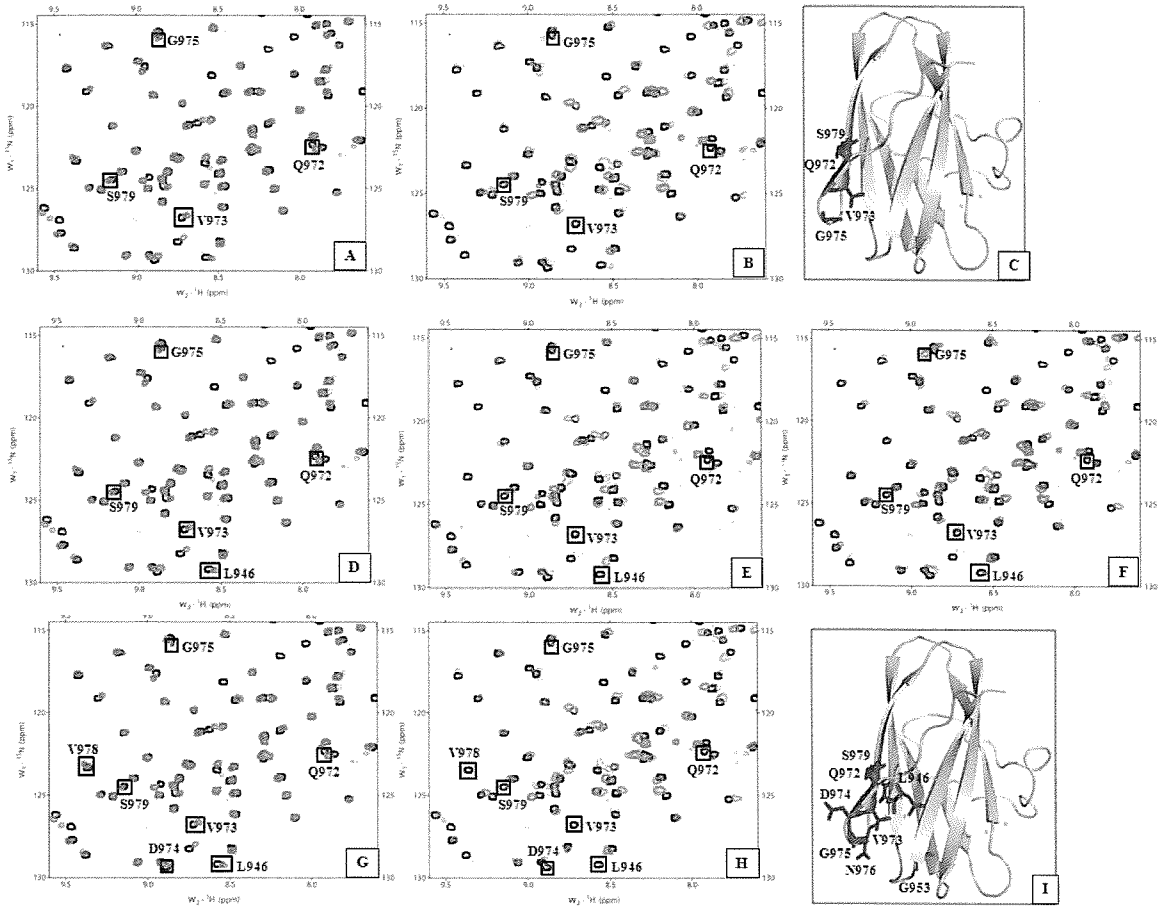
G975
Q972
S979
V973
A
B
S979
Q972
V978
G975
C
L946
D
E
F
V978
D974
G
H
S979
Q972
L946
D974
V973
G975
N976
G953
I

Figure 7

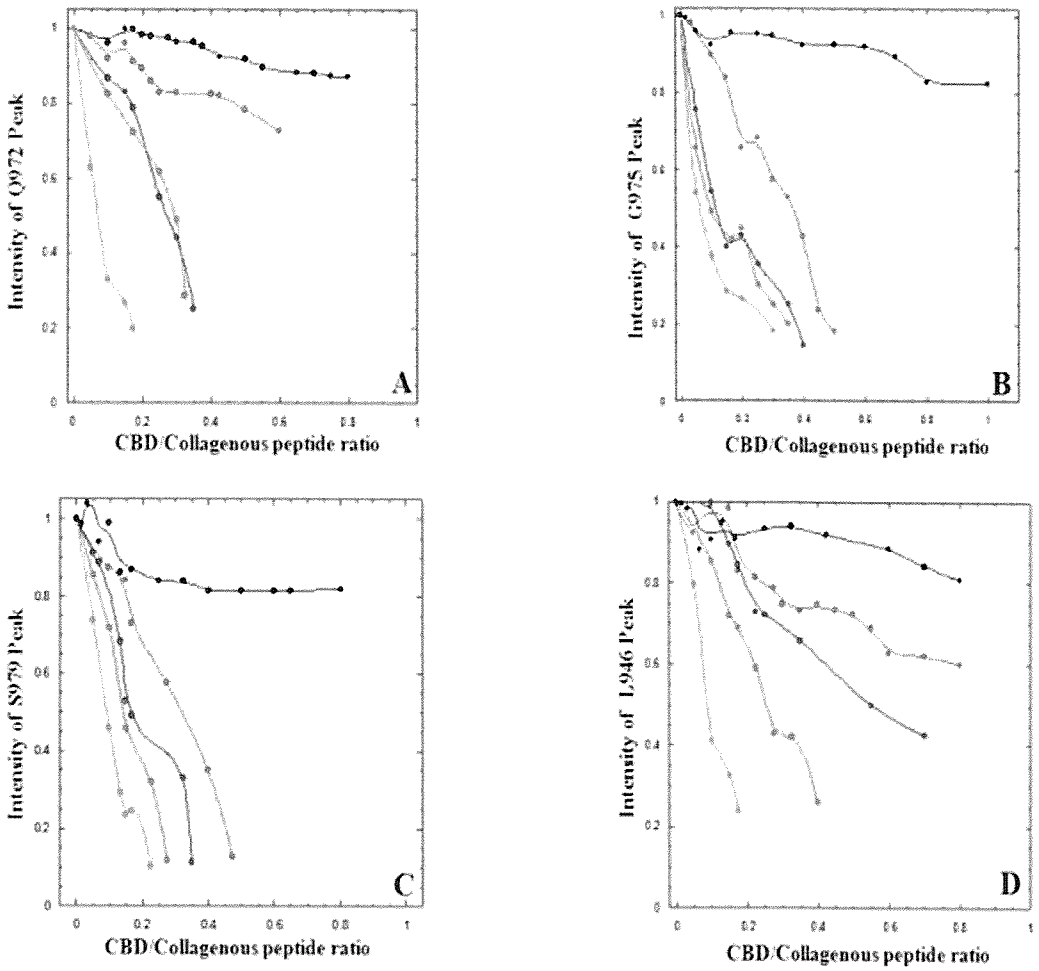
Intensity of Q972 Peak
CBD/Collagenous peptide ratio
A
Intensity of Q975 Peak
CBD/Collagenous peptide ratio
B
Intensity of S979 Peak
CBD/Collagenous peptide ratio
C
Intensity of L946 Peak
CBD/Collagenous peptide ratio
D

Figure 8

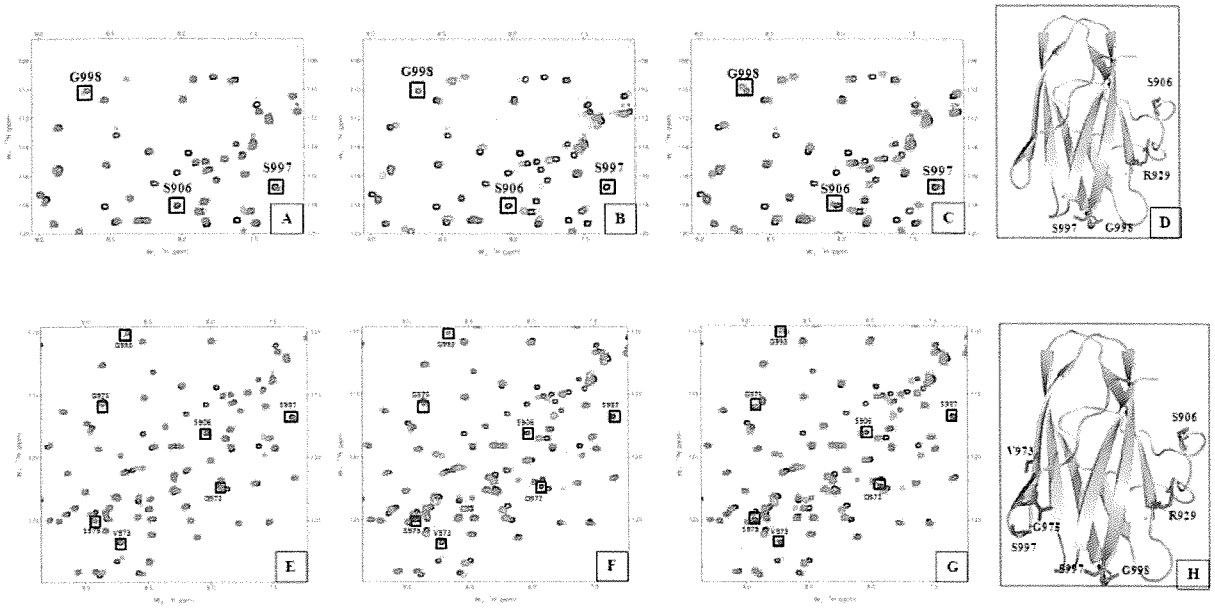
G998
S997
S906
A
G998
S997
S906
B
G998
S997
S906
C
S906
R929
S997
G975
D
E
F
G
S906
V973
G975
R929
S997
G998
H

Figure 9

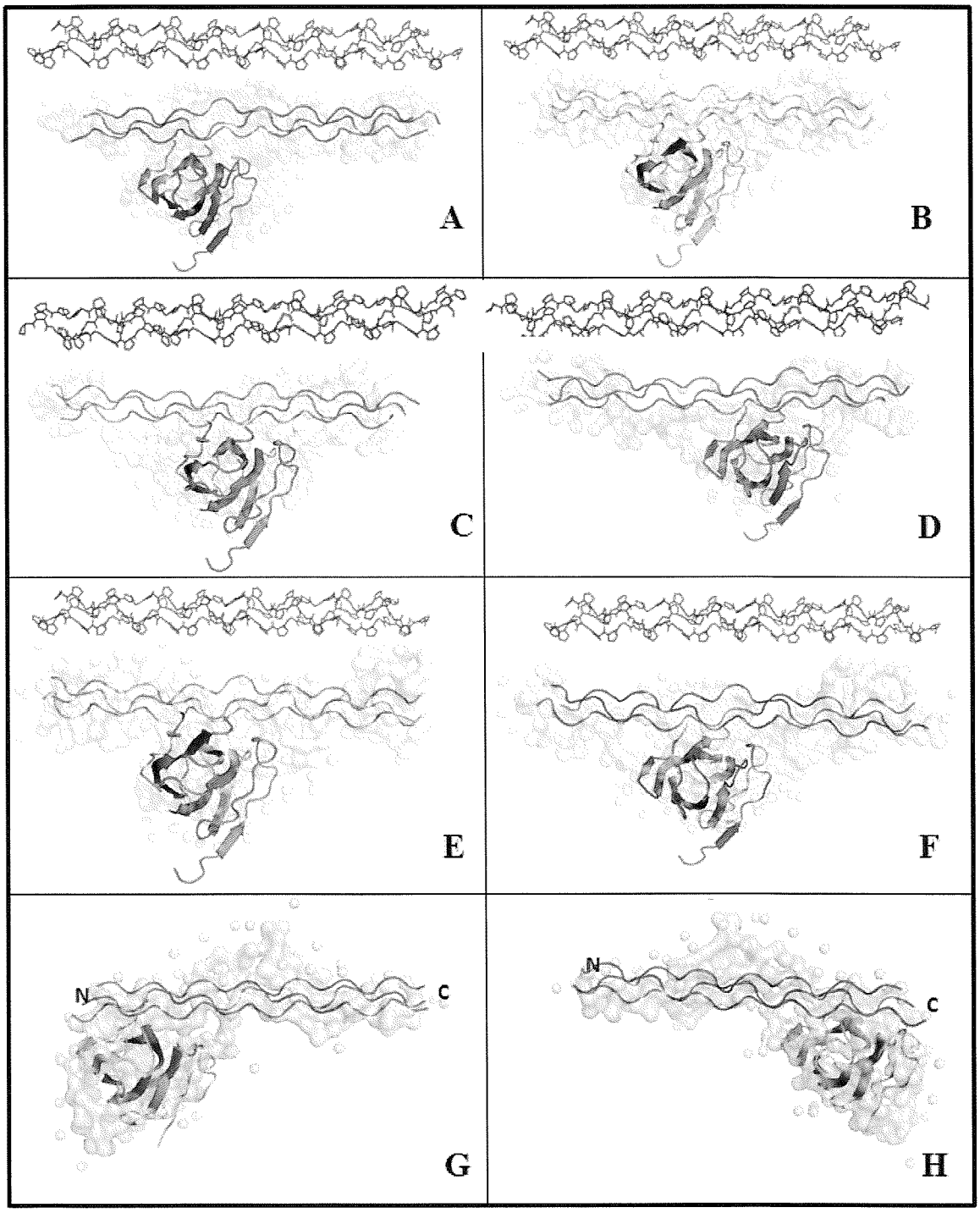

Figure 10

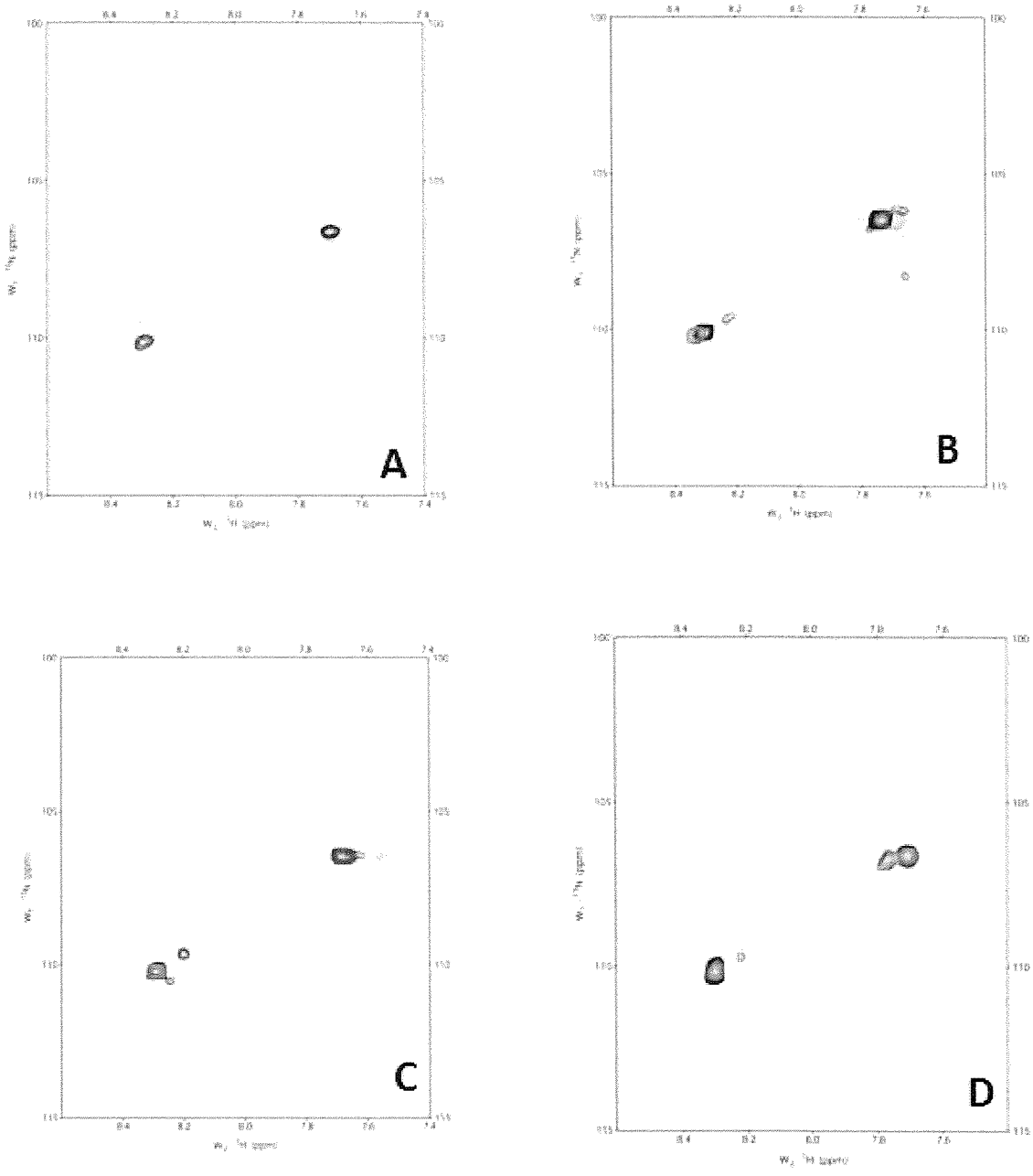

Figure 11

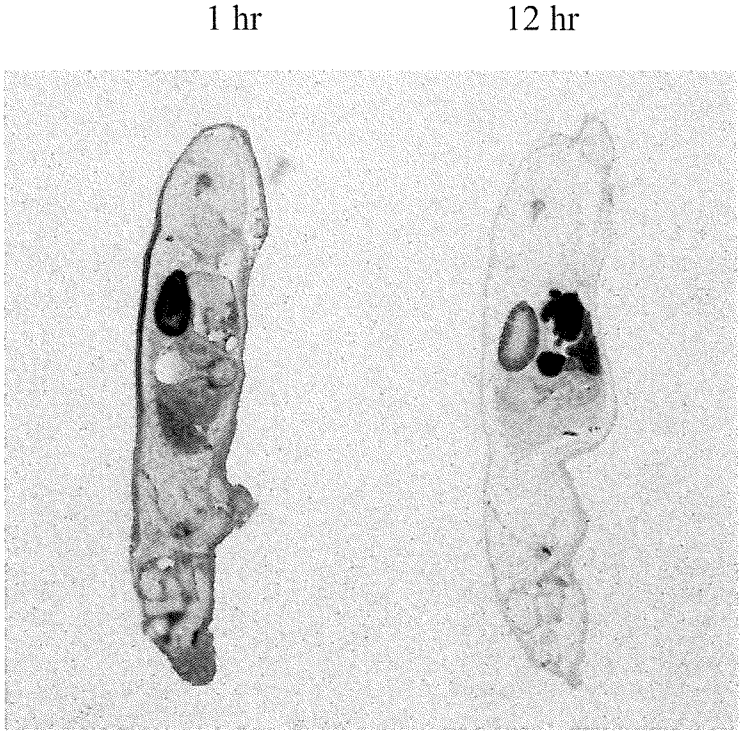

Figure 12

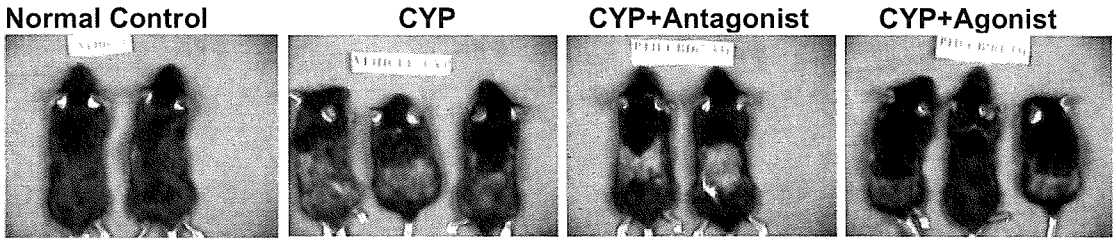

Figure 13

A) Normal Control

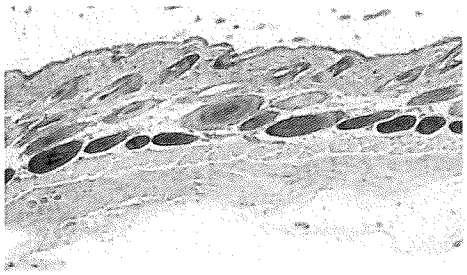

B) CYP

C) CYP + Agonist

D) CYP + Antagonist

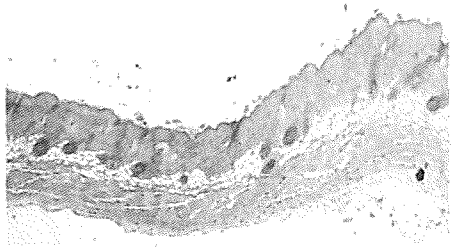

Figure 14

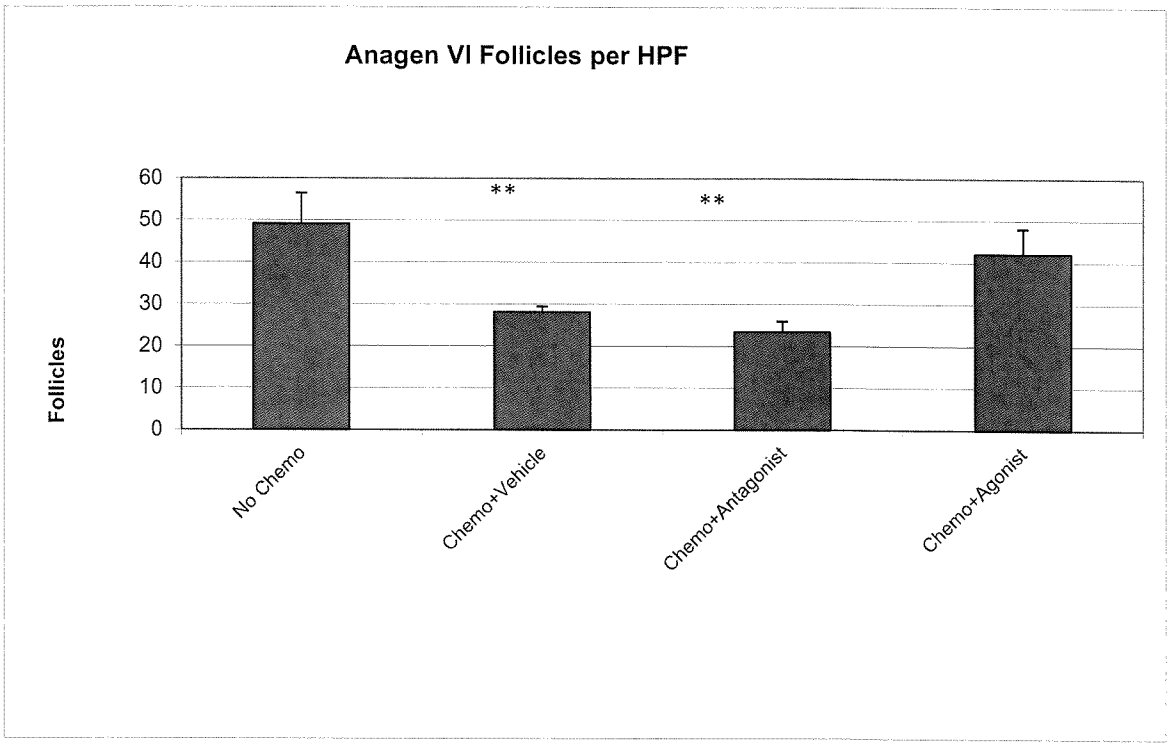
Anagen VI Follicles per HPF
Follicles
60
50
40
30
20
10
0
**
**
No Chemo
Chemo+Vehicle
Chemo+Antagonist
Chemo+Agonist

Figure 15

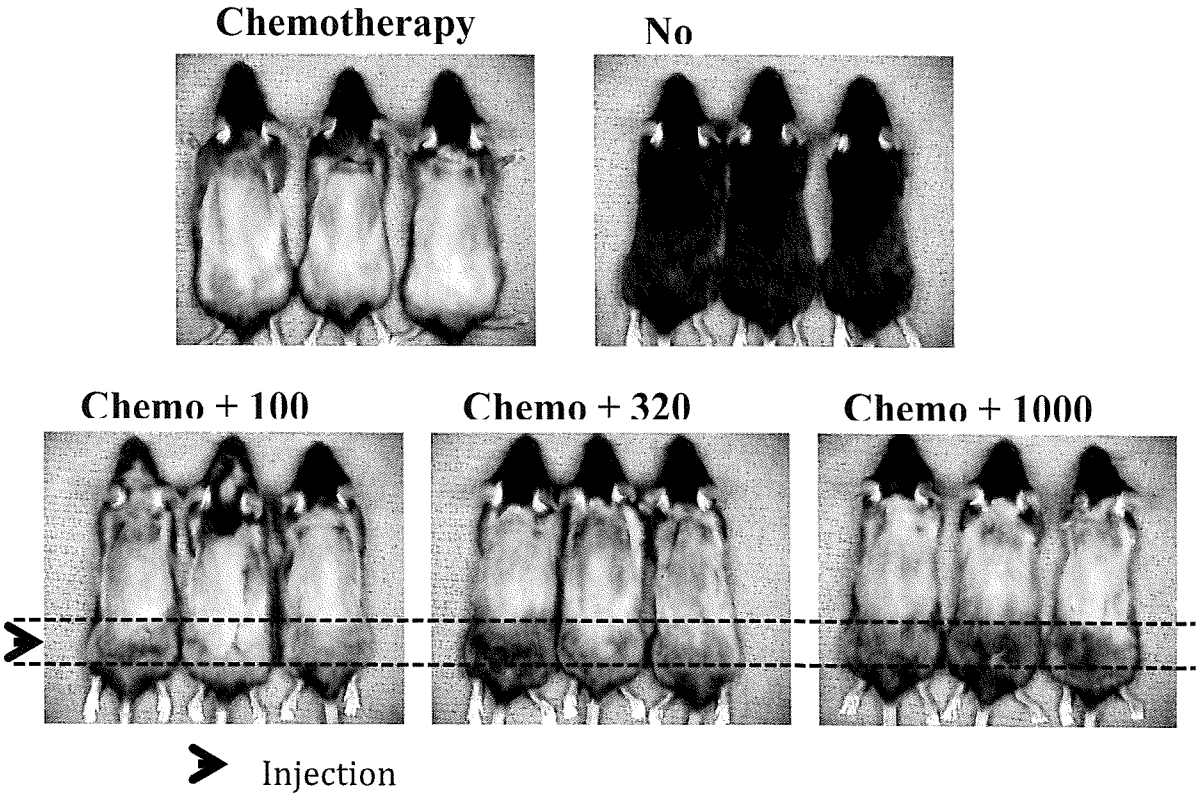
Chemotherapy
No
Chemo + 100
Chemo + 320
Chemo + 1000
Injection

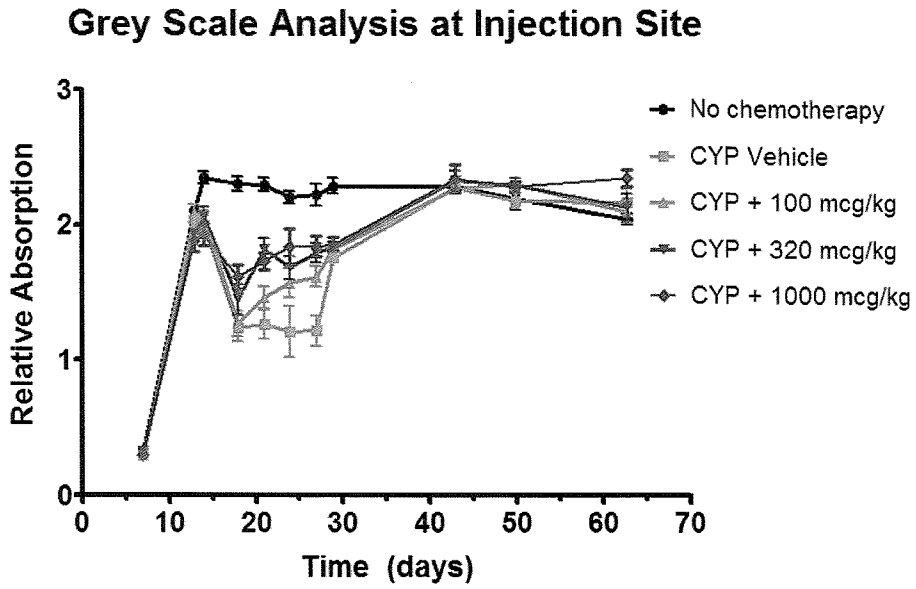
Grey Scale Analysis at Injection Site
Relative Absorption
Time (days)
No chemotherapy
CYP Vehicle
CYP + 100 mcg/kg
CYP + 320 mcg/kg
CYP + 1000 mcg/kg
0
1
2
3
0
10
20
30
40
50
60
70

Figure 16

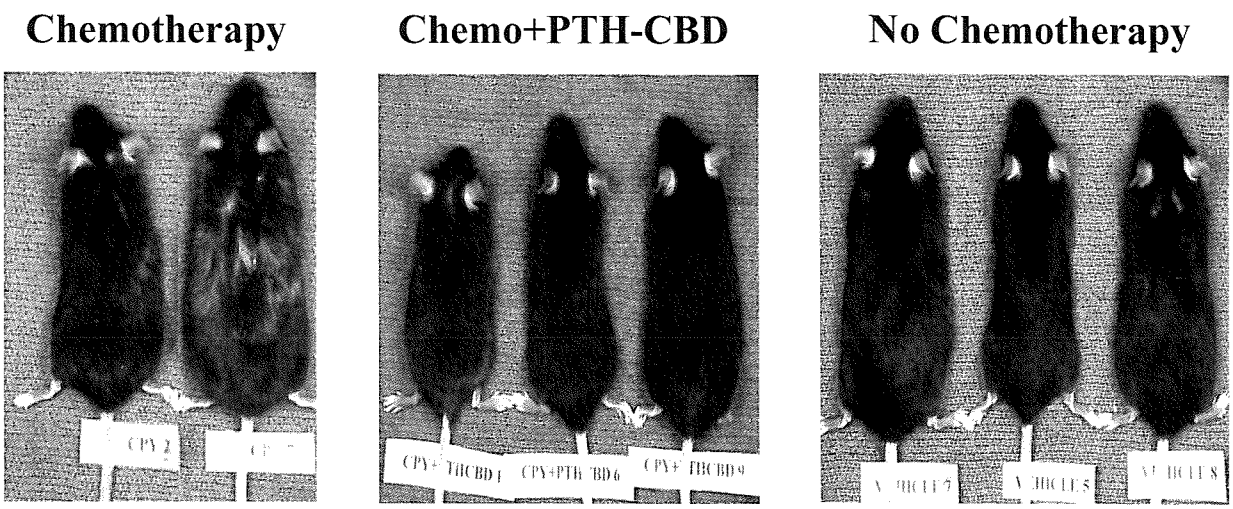

Figure 17

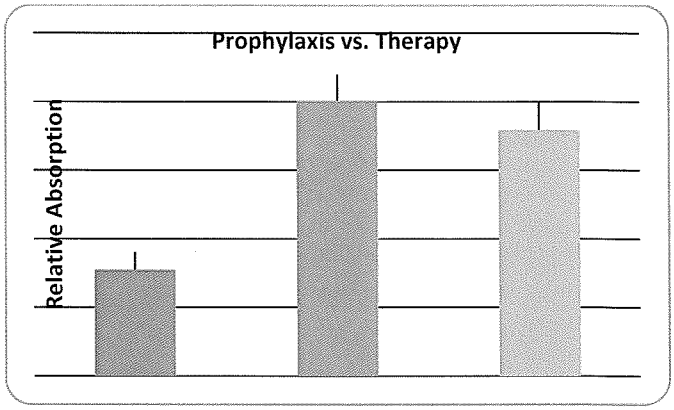
Prophylaxis vs. Therapy
Relative Absorption

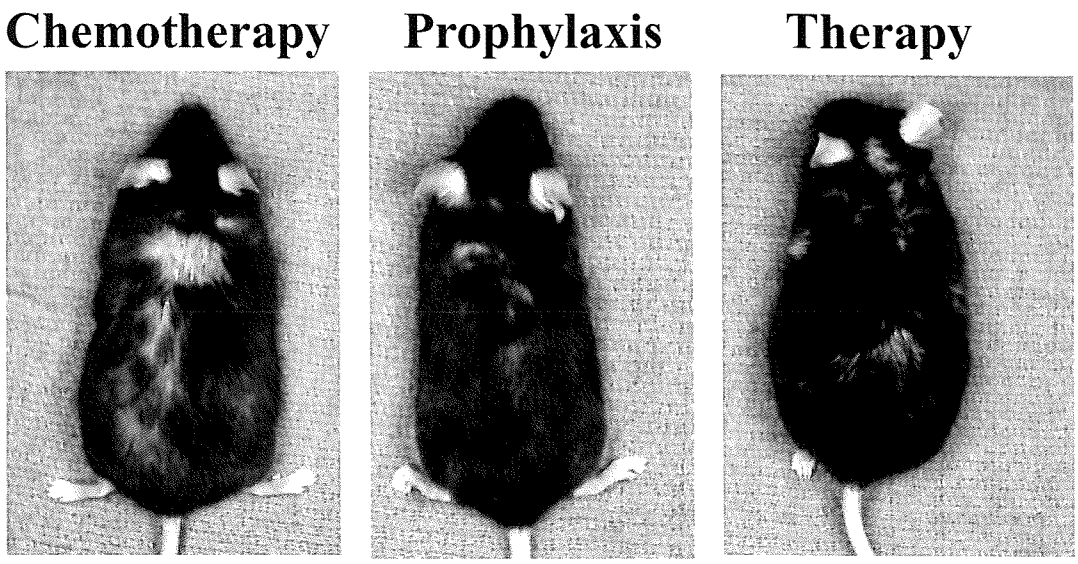
Chemotherapy
Prophylaxis
Therapy

Figure 18

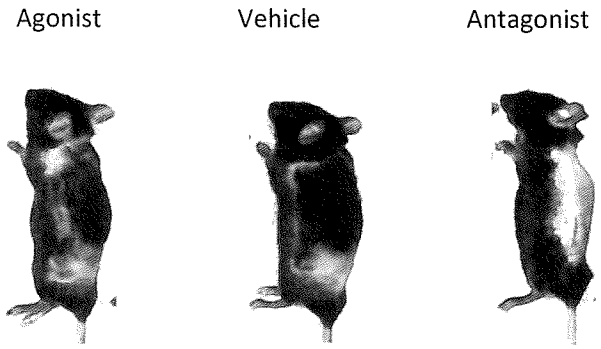

Figure 19

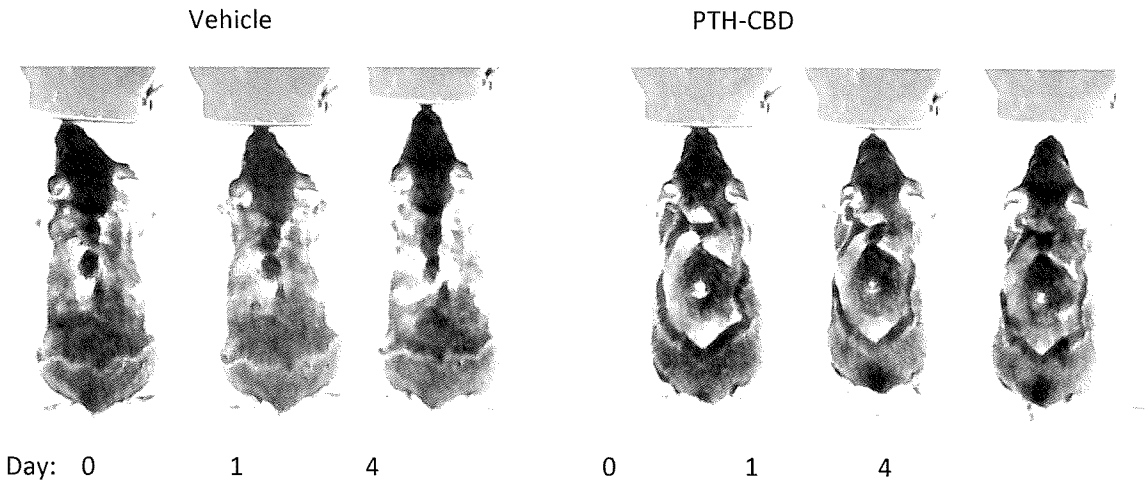

Figure 20

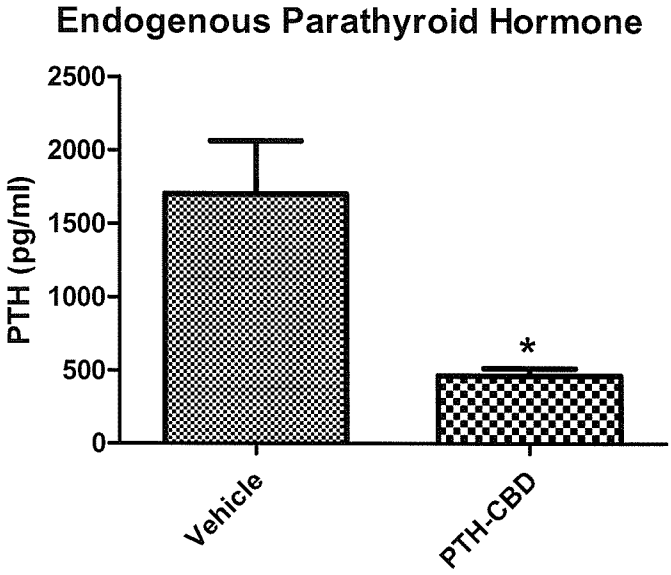
Endogenous Parathyroid Hormone
PTH (pg/ml)
2500
2000
1500
1000
500
0
*
Vehicle
PTH-CBD